frontiers in Earth Science

ORIGINAL RESEARCH
published: 03 August 2021
doi: 10.3389/feart.2021.692895

The Nitrogen Cycle in an Epeiric Sea in the Core of Gondwana Supercontinent: A Study on the Ediacaran-Cambrian Bambuí Group, East-central Brazil

Paula Luiza Fraga-Ferreira[1], Magali Ader[2], Sérgio Caetano-Filho[1], Pierre Sansjofre[3], Gustavo Macedo Paula-Santos[4], Marly Babinski[1], Cristian Guacaneme[1], Carolina Bedoya-Rueda[1], Virginia Rojas[2], Humberto L. S. Reis[5], Matheus Kuchenbecker[6] and Ricardo I. F. Trindade[7]*

[1]Instituto de Geociências, Universidade de São Paulo, São Paulo, Brazil, [2]Université de Paris, Institut de Physique du Globe de Paris, CNRS, Paris, France, [3]Institut de Minéralogie, de Physique des Matériaux et de Cosmochimie, MNHN, Sorbonne Université, Paris, France, [4]MARUM – Center for Marine Environmental Sciences, University of Bremen, Bremen, Germany, [5]Laboratório de Modelagem Tectônica, Departamento de Geologia, Universidade Federal de Ouro Preto, Ouro Preto, Brazil, [6]Laboratório de Estudos Tectônicos, Centro de Estudos em Geociências, Instituto de Ciência e Tecnologia, Universidade Federal do Vale do Jequitinhonha e Mucuri, Diamantina, Brazil, [7]Instituto de Astronomia, Geofísica e Ciências Atmosféricas, Universidade de São Paulo, São Paulo, Brazil

OPEN ACCESS

Edited by:
Graham Shields,
University College London,
United Kingdom

Reviewed by:
Xinqiang Wang,
China University of Geosciences,
China
Fabricio Caxito,
Federal University of Minas Gerais,
Brazil

***Correspondence:**
Paula Luiza Fraga-Ferreira
paulafraga@usp.br

Specialty section:
This article was submitted to Geochemistry, a section of the journal Frontiers in Earth Science

Received: 09 April 2021
Accepted: 26 July 2021
Published: 03 August 2021

Citation:
Fraga-Ferreira PL, Ader M, Caetano-Filho S, Sansjofre P, Paula-Santos GM, Babinski M, Guacaneme C, Bedoya-Rueda C, Rojas V, Reis HLS, Kuchenbecker M and Trindade RIF (2021) The Nitrogen Cycle in an Epeiric Sea in the Core of Gondwana Supercontinent: A Study on the Ediacaran-Cambrian Bambuí Group, East-central Brazil. Front. Earth Sci. 9:692895. doi: 10.3389/feart.2021.692895

The Ediacaran-Cambrian transition is marked by the diversification of metazoans in the marine realm. However, this is not recorded by the Ediacaran-Cambrian Bambuí Group of the São Francisco basin, Brazil. Containing the sedimentary record of a partially confined foreland basin system, the Bambuí strata bear rare metazoan remnants and a major carbon isotope positive excursion decoupled from the global record. This has been explained by changes in the paleogeography of the basin, which became a restricted epicontinental sea in the core of the Gondwana supercontinent, promoting episodes of shallow water anoxia. Here, we report new $\delta^{15}N_{bulk}$ data from the two lowermost second-order transgressive-regressive sequences of the Bambuí Group. The results show a rise of $\delta^{15}N$ values from +2 to +5‰ in the transgressive system tract of the basal sequence, which was deposited when the basin was connected to other marginal seas. Such excursion is interpreted as an oxygenation event in the Bambuí sea. Above, in the regressive systems tract, $\delta^{15}N$ values vary from +2 to +5‰, pointing to instabilities in the N-cyle that are concomitant with the onset of basin restrictions, higher sedimentary supply/accommodation ratios, and the episodic anoxia. In the transgressive systems tract, the $\delta^{15}N$ values stabilise at ~+3.5‰, pointing to the establishment of an appreciable nitrate pool in shallow waters in spite of the basin full restriction as marked by the onset of a positive carbon isotope excursion. In sum, our data show that the N-cycle and its fluctuations were associated with variations in sedimentary supply/accommodation ratios induced by tectonically-related paleogeographic changes. The instability of the N-cycle and redox conditions plus the scarcity of nitrate along regression episodes might have hindered the development of early benthic metazoans within the Bambuí seawater

and probably within other epicontinental seas during the late Ediacaran-Cambrian transition.

Keywords: nitrogen isotopes, paleoenviroments, Bambuí Group, Ediacaran-Cambrian, epeiric sea, chemostratigraphy

INTRODUCTION

Nitrogen (N) has two stable isotopes, ^{14}N and ^{15}N, and they occur in a proportion of 99.633 and 0.337%, respectively (Meija et al., 2016). Due to its abundance, ability to build chemical bonds with carbon, and to join redox reactions when it is dissolved in liquid water, nitrogen is an important component in Earth's life system (Stüeken et al., 2016). In seawater, N is found mostly as N_2 (di-nitrogen), NO_2^- (nitrite), NO_3^- (nitrate), NH_4^+ (ammonium) and N_{org} (dissolved or particulate organic nitrogen) (Thomazo et al., 2011) depending on the redox structure of the water column, which controls most of the reactions operating the N-biogeochemical cycle. These reactions impart nitrogen isotope fractionation, hence, they also control the nitrogen isotope composition of these nitrogen species. Based on the study of modern systems, it is commonly assumed that the measured $\delta^{15}N$ of a rock/sediment reflects the isotopic signature of primary producers (i.e. superficial waters) which itself reflects the $\delta^{15}N$ of the N species they have assimilated (*see* review in Ader et al., 2016). Hence, $\delta^{15}N$ in past sedimentary rocks enables to obtain valuable information about changes in both redox structure of ancient water bodies (e.g., Godfrey and Falkowski, 2009; Quan et al., 2013; Ader et al., 2014; Wang et al., 2015; Chen et al., 2019) and past N-biogeochemical cycle paths (e.g., Cremonese et al., 2013; Stüeken et al., 2015; Cox et al., 2019; Sun et al., 2019; Xu et al., 2020).

To understand the biogeochemical cycle of nitrogen in the past, it is important to understand how it operates now, since, even if not accurate, our knowledge of the modern N cycle is used as the basis of comparison to understand ancient systems. When they are not completed, the reactions of this cycle produce isotopic fractionation ($\varepsilon = \delta^{15}N_{product} - \delta^{15}N_{reactant}$) and the modern biogeochemical cycle of N in the oceans operates as follows (**Figure 1**):

i) Nitrogen enters the ocean when N_2 is fixed by bacteria and archaea, the diazotrophs (ε = −7 to +1‰, Zhang et al., 2014; Sigman and Fripiat, 2019). Subsequently, N_2 is converted to a biologically available form of N, the NH_3 gas, which is quickly converted to the soluble NH_4^+ (Glass et al., 2009). The fractionation on this step depends strongly on which cofactor is used by the nitrogenase enzyme. Mo-based nitrogenase imparts a small fractionation (−2 to +1‰), while Fe or V-based ones lead to a much larger isotopic differentiation, reaching values as low as −7‰ (Zhang et al., 2014).

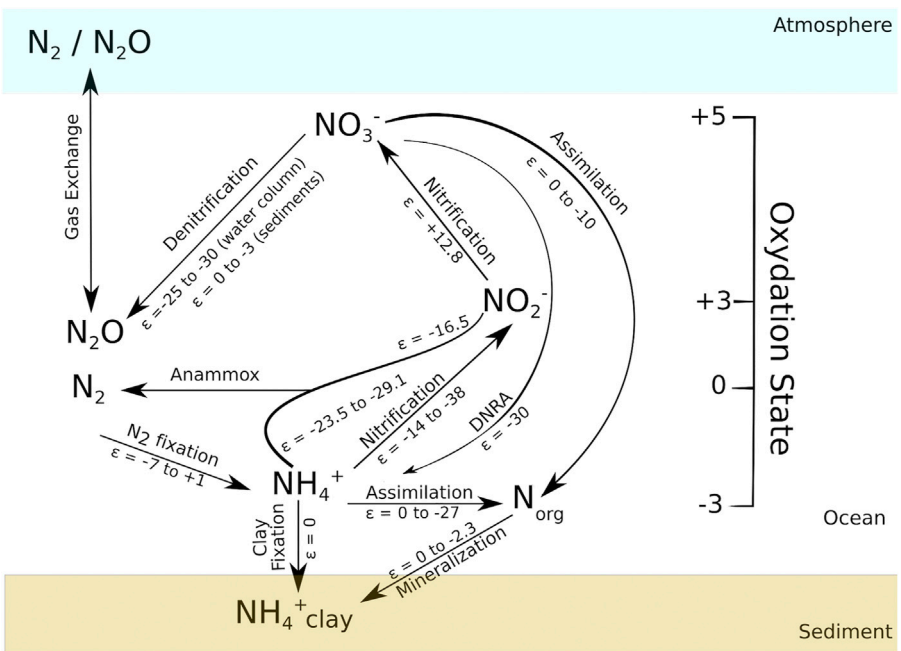

FIGURE 1 | Schematic diagram of the modern marine nitrogen cycle. Oxidation state of nitrogen species is shown on the vertical axis going from −3 (NH_4^+) to +5 (NO_3^-). Nitrogen isotopic fractionation of the pathways of the N-cycle are detailed in the text and are expressed in ‰. Modified after Ader et al. (2016).

ii) During organic matter mineralization, N_{org} is converted into NH_4^+ (ε = 0 to −2.3‰, Möbius, 2013). This NH_4^+ can be fixed into clays (ε = 0, Ader et al., 2016), since its ionic radius is similar to the potassium one (Müller, 1977; Greenfield, 1992) or it can be assimilated by organisms (ε = 0 to −27‰, Hoch et al., 1992; Pennock et al., 1996; Liu et al., 2013). NH_4^+ can also be nitrified, i.e. NH_4^+ is oxidized to NO_2^- (ε = −14 to −38‰, Casciotti, 2009) and NO_2^- is rapidly oxidized to NO_3^- (ε = +12.8‰, Casciotti, 2009). Finally, NH_4^+ can contribute to the loss of fixed N in the ocean in a process called anammox, in which NO_2^- is used to oxidize NH_4^+, generating N_2 (ε = −23.5 to −29.1‰ for $\varepsilon_{NH_4^+ - N_2}$ and ε = −16.5‰ for $\varepsilon_{NO_2^- - N_2}$, Brunner et al., 2013).

iii) Denitrification (ε = −25 to −30‰ in the water column and 0 to −3‰ in sediments, Granger et al., 2008; Casciotti, 2009; Kessler et al., 2014), the conversion of NO_3^- to N_2/N_2O, is the major sink of fixed N in modern oceans. It occurs in the sediments and in the water column where oxygen levels are low. The remarkable difference in the fractionation of N in the two environments where the process happens is explained by the fact that in sediment pore waters nitrate is almost fully consumed, leading to a small fractionation (Sigman and Fripiat, 2019). NO_3^- is an important nutrient, accounting for most of the fixed N in marine ecosystems. When it is assimilated by microorganisms (ε = 0 to −10‰, Casciotti, 2009; Granger et al., 2010) its fractionation depends on the abundance of the species, the scarcer is the nutrient, the closer to 0‰ the kinetic isotopic effect is (Fogel and Cifuentes, 1993).

iv) The direct conversion of NO_3^- to NH_4^+, known as dissimilatory nitrate reduction to ammonium (DNRA). Although the isotopic effect of this process is not very well known, it can account for fractionations larger than −30‰ (McCready et al., 1983).

Many sedimentary basins worldwide record the transition from the Ediacaran to Cambrian with a rich fossil assemblage, however this does not happen in the Bambuí Group, east-central Brazil, which is almost fossil-barren. This Neoproterozoic unit is situated in the São Francisco Craton and was deposited in a foreland basin, which was generated in response to the uplift of the Brasília and Aracuaí belts (Reis et al., 2017). The Bambuí Group encompasses carbonates and siliciclastic rocks that were deposited above glaciogenic units (Alkmim and Martins-Neto, 2001, 2012; Martins-Neto and Hercos, 2002; Martins-Neto, 2009; Reis and Alkmim, 2015) and lately, it has been a matter of intense research regarding the conditions that could have prevented the Ediacaran fauna to thrive at the core of West Gondwana (e.g., Paula-Santos et al., 2017, 2020; Uhlein et al., 2017, 2019; Okubo et al., 2018, 2020; Paula-Santos and Babinski, 2018; Caetano-Filho et al., 2019, 2021; Crockford et al., 2019). Geochronological and chemostratigraphic data suggest that the Bambuí evolved from a sea connected to the global ocean to a fully restricted environment (Paula-Santos et al., 2015, 2017), which might have influenced its paleoenvironmental conditions, leading to very high $\delta^{13}C_{carb}$ values (Iyer et al., 1995; Martins and Lemos, 2007; Kuchenbecker et al., 2016b; Guacaneme et al., 2017; Caetano-Filho et al., 2019; Uhlein et al., 2019) and anoxia (Paula-Santos et al., 2017; Hippertt et al., 2019; Uhlein et al., 2019). These in turn may have prevented complex life forms to thrive (Hippertt et al., 2019). Further knowledge on the interplay between the redox state of Bambuí seawater and the biological metabolic paths could help understanding the limiting conditions for life during the Ediacaran-Cambrian boundary, and thus on the comprehension of how life may have progressed to more complex forms at that period. Aiming to contribute to this debate, we present a new redox proxy on the Bambuí Group sediments: nitrogen isotopic composition ($\delta^{15}N$). The nature of $\delta^{15}N$ data have the potential to provide important information on the Bambuí seawater chemistry, its redox state and prevailing metabolisms.

GEOLOGICAL SETTING

The São Francisco Basin and the Bambuí Group

The São Francisco Basin (SFB) is a long-lasting sedimentary locus in east-central Brazil, whose records cover a large area (~350.000 km^2) of the São Francisco craton (**Figure 2**). This intracratonic basin encompasses many first order sedimentary cycles younger than 1.8 Ga, which record important tectonic and climate events (Reis et al., 2017). The basement of SFB present three main structural domains: two structural highs, named Januária (north) and Sete Lagoas (south) highs, separated by a deep NW-trending aulacogen, called Pirapora aulacogen. During the Neoproterozoic-Phanerozoic transition, the SFB hosted a complex foreland system, which evolved in response to the growth of the Brasília and Araçuaí orogens around the São Francisco craton in the context of the Gondwana supercontinent assembly (e.g. Alkmim and Martins Neto, 2001; Martins-Neto, 2009; Reis and Suss, 2016; Reis et al., 2017; Uhlein et al., 2017; Kuchenbecker et al., 2020). The records of such important foreland system are encompassed in the Bambuí Group, which cover a large area of the São Francisco basin, presenting mostly carbonates, pelites, sandstones and conglomerates. Regarding the lithostratigraphy of the Bambuí Group, Dardenne (1978), after Costa and Branco (1961), divided the unit into six units: A diamictite at its base and the Sete Lagoas, Serra de Santa Helena, Lagoa do Jacaré, Serra da Saudade and Três Marias formations. Other units of the Bambuí Group are the Samburá (Barbosa et al., 1970), Lagoa Formosa (Seer et al., 1989) and Gorutuba formations (Kuchenbecker et al., 2016a). The Bambuí has been interpreted as a first-order sequence subdivided into four second-order progradational-retrogradational sequences (**Figure 3**) (Martins and Lemos 2007; Martins-Neto, 2009; Reis and Alkmim, 2015; Caetano-Filho et al., 2019). The basal second-order sequence comprises the Carrancas Formation and the base of the Sete Lagoas Formation. The Carrancas Formation is composed of conglomerates with a sandy-calcareous matrix, whose glacial origin has been discussed (e.g. Martins-Neto et al., 2001; Uhlein et al., 2016; Delpomdor et al., 2020) and the overlying Sete Lagoas Formation consists mainly of marine dolostones, limestones and organic-rich shales (e.g. Iglesias and Uhlein, 2009; Reis and Suss, 2016). The basal limestones of the Sete Lagoas Formation have been interpreted as

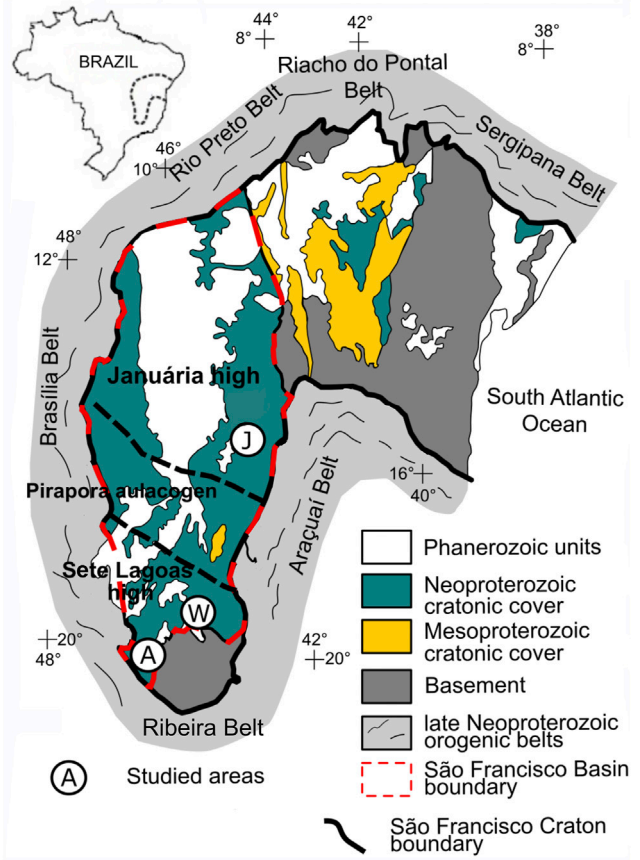

FIGURE 2 | The São Francisco Craton geological map and the São Francisco Basin. Studied sections: A, Arcos; W, Well 1; J, Januária. Modified after Caetano-Filho et al. (2019).

a cap carbonate related to a Neoproterozoic glaciation (e.g. Babinski et al., 2007; Vieira et al., 2007b; Caxito et al., 2012; Kuchebecker et al., 2016a). The two-following second-order sequences are the upper part of the Sete Lagoas, Serra de Santa Helena, Lagoa do Jacaré, and the lower Serra da Saudade formations, which also record marine environments. The Serra de Santa Helena Formation is composed of siltites, pelites, shales and minor limestones, whereas the Lagoa do Jacaré Formation is characterized by pisolitic and oolitic limestones, marbles, intraclastic breccias, shales and siltites and the Serra da Saudade Formation is a succession of siltites and greenish shales, with minor limestones and dolostones (Dardenne, 1978). The uppermost second-order sequence encompasses the upper Serra da Saudade and the shallow marine/continental deposits of the Três Marias and Gorotuba formations (Kuchenbecker et al., 2016a; Reis and Suss, 2016). At the western portion of the basin, the Samburá and Lagoa Formosa formations are interpreted as the deposits of fan-deltas and submarine-fans, representing the gravitational flows associated to the intermediate second-order sequences (Uhlein et al., 2011; Reis et al., 2017).

Chemo and Sequence Stratigraphy of the Bambuí Group

Many chemostratigraphic studies were done on the Bambuí Group applying ^{13}C isotopes on carbonate rocks ($\delta^{13}C_{carb}$) (Iyer et al., 1995; Santos et al., 2004; Martins and Lemos, 2007; Vieira et al., 2007a; Caxito et al., 2012; Kuchenbecker et al., 2016b; Guacaneme et al., 2017; Paula-Santos et al., 2017; Caetano-Filho et al., 2019; Uhlein et al., 2019). Considering $\delta^{13}C_{carb}$ and also $^{87}Sr/^{86}Sr$ ratios, Paula-Santos et al. (2017) divided the basal Bambuí into three chemostratigraphic intervals (CIs) and interpreted the shifts in the measurements in terms of oceanic connection and restriction of the basin (**Figure 3**). The first interval (CI-1) comprises the Sete Lagoas cap carbonates, in which $\delta^{13}C_{carb}$ values records a negative excursion (−3 to −5‰) followed by a positive excursion (−5 to 0‰). Also, at CI-1, the $^{87}Sr/^{86}Sr$ ratio increases from 0.7074 to 0.7082. At CI-2, which corresponds to the middle of the Sete Lagoas Formation, both $\delta^{13}C_{carb}$ and $^{87}Sr/^{86}Sr$ are stable, around 0‰ and 0.7082, respectively. At the CI-2 the marine late Ediacaran index fossil *Cloudina sp*. (Grotzinger et al., 1995) was reported by Warren et al. (2014), suggesting that the São Francisco basin was connected to other Gondwana marine basins through a sea pathway, allowing the migration of metazoans and C-isotope homogenization with global seawater. Finally, the third interval (CI-3), encompasses the upper Sete Lagoas, Serra de Santa Helena, and Lagoa do Jacaré formations. At CI-3, $\delta^{13}C_{carb}$ reaches very high values (up to +16‰) and $^{87}Sr/^{86}Sr$ ratios decrease when compared to CI-2, being close to 0.7075. The reported $^{87}Sr/^{86}Sr$ ratios are low for the late Ediacaran/early Cambrian, suggesting restriction and lack of homogenization with external seawaters, hence, its Sr signature was mostly controlled by weathering of ancient carbonate platforms (Paula-Santos et al., 2015, 2017). Such restriction was probably caused by the progressive uplift of the marginal orogens of the São Francisco Craton (Paula-Santos et al., 2017), which isolated the basin. Uhlein et al. (2019) named these very high $\delta^{13}C_{carb}$ values reported in CI-3 interval as MIBE (Middle Bambuí Excursion). They were mostly interpreted as the result of enhanced burial of organic matter and active methanogenesis coupled to methane emissions to the atmosphere (Iyer et al., 1995; Paula-Santos et al., 2017; Caetano-Filho et al., 2021) or the consequence of a change in carbon input due to weathering of ancient sedimentary carbonates and higher burial rates of authigenic carbonates due to organic matter oxidation (Uhlein et al., 2019; Cui et al., 2020). The chemostratigraphic division made by Paula-Santos et al. (2017) was later corroborated by Paula-Santos et al. (2018) since the Rare Earth Elements + Yttrium (REY) patterns that were reported by the authors present secular trends that matches the intervals CI-1, CI,-2 and CI-3. Using geochemical data and two major stratigraphic surfaces, the maximum flooding surface (MFS) and the first sequence boundary (SB1), which are recognizable throughout the basin, Caetano-Filho et al. (2019) established correlations between the sections used in this work, classifying its basal units in terms of systems tracts identified both at the Sete Lagoas and at the Januária highs. The authors defined a transgressive system tract (TST), an early highstand system tract

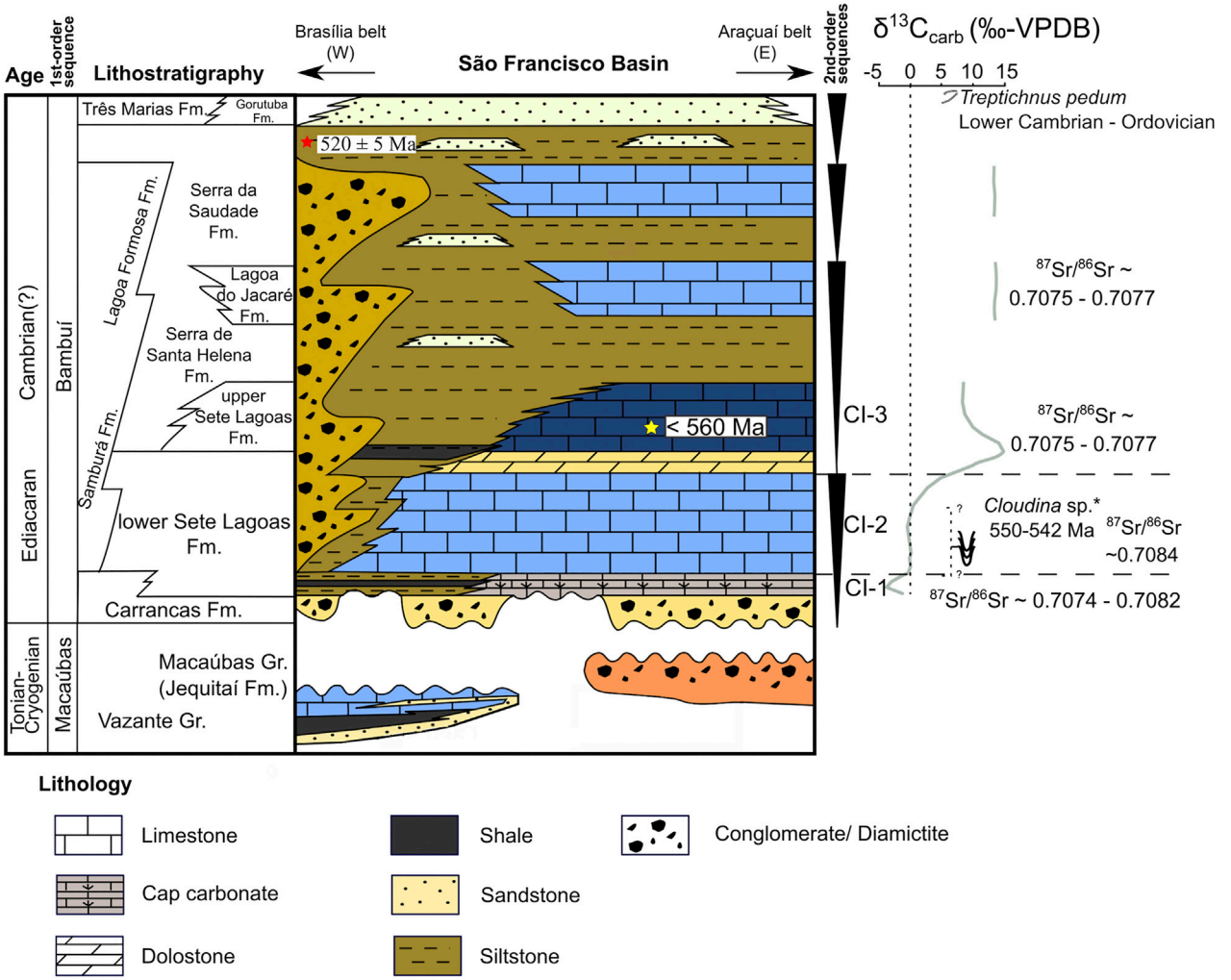

FIGURE 3 | Litho-sequence and chemostratigraphy of the São Francisco Basin. Yellow Star represents maximum depositional age obtained in detrital zircons in the upper Sete Lagoas Formation (Paula-Santos et al., 2015); The red star represents a Serra da Saudade Concordia Age obtained by Moreira et al. (2020). Chemostratigraphic intervals (CIs) were defined by Paula-Santos et al. (2017). Cloudina occurrences are reported in Warren et al. (2014) and Perrella Júnior et al. (2017) and *Treptichnus pedum* occurrences are reported in Sanchez et al. (2020). Modified after Caetano-Filho et al. (2019).

(EHST) and a late highstand system tract (LHST) and also a second transgression at the base of the upper second-order sequence. The TST corresponds to a retrogradational pattern that marks a transgression over the forebulge of the Bambuí domain and its connection to the global ocean, and it comprises deposits of diamictites from Carrancas and carbonates from the basal Sete Lagoas Formation. This sequence ends at MFS, which in the Sete Lagoas High is marked by a succession of shale and mudstones, whilst in Januária bindstones lacking structures related to flows were chosen as the limiting surface, this interval is associated to the CI-1 of Paula-Santos et al. (2017). Above it, a progradational pattern shows that a regression occurred, marking the EHST. At this stage, the Bambuí was still connected to the global ocean. Carbonates are the main lithology of this stage and represent a stable marine ramp. The boundary between EHST and LHST was defined by a sharp increase in the Sr/Ca ratio since the latter present an average value of 0.004, while the former the value of 0.001 and this increment was interpreted as the beginning of the restriction of the Bambuí seaway. LHST comprises very pure carbonates that become coarser towards the top of the sequence. Despite the rise in Sr/Ca ratios, Paula-Santos et al. (2017) defined that the CI-2 covers both EHST and LHST, which places the beginning of the restriction later than it was suggested by Caetano-Filho et al. (2019). The LHST ends with the surface identified as SB1 marking the beginning of the second second-order sequence, which corresponds to the CI-3 of Paula-Santos et al. (2017). The SB1 is defined by subaerial features in shallow environments, whereas in deeper it is defined by an erosional surface at the base of peritidal channels limestones.

Age of the Bambuí Group

A large set of data show that the deposition of the Bambuí Group largely took place between the late Ediacaran and Cambrian. Paula-Santos et al. (2015) determined U-Pb ages in detrital zircons from pelites intercalated with carbonates from the upper part of the Sete Lagoas Formation and obtained a maximum depositional age around 560 Ma. The discovery of fossils of *Cloudina sp*. and *Corumbella Werneri* (550–542 Ma) (Grotzinger et al., 1995) in the middle Sete Lagoas Formation (Warren et al., 2014; Perrella Júnior et al., 2017) corroborate Paula-Santos et al. (2015) ages. Recently, Moreira et al. (2020) reported that ten prismatic zircon grains extracted from a K-bentonite volcanoclastic bed in the upper Serra da Saudade Formation defined a U-Pb Concordia age of 520 Ma ± 5 Ma. Finally, the fossil *Treptichnus pedum* was reported in the upper Três Marias formation, which places the deposition age of this unit in the early Paleozoic (Sanchez et al., 2020).

MATERIALS AND METHODS

Studied Sections

Three stratigraphic sections from the Bambuí Group were studied in this work: Januária (~130 m-thick), an assemblage of three minor sections in the central-east portion of the São Francisco Basin in Januária High domain, Arcos (180 m-thick) and Well 1 (430 m-thick), the latter two sections corresponding to drill cores, at the South of the Basin, in the Sete Lagoas High domain (**Figure 2**). Januária and Arcos represent shelf environments of the Bambuí, while Well 1 represents a forebulge graben setting. For detailed lithostratigraphy and sedimentological features of Januária, Arcos and Well 1, *see* Caetano-Filho et al. (2019), Kuchenbecker et al. (2011, 2013) and Reis and Suss (2016), respectively. The samples analyzed here correspond to the two lowermost second-order sequences of the Bambuí Group.

Januária Section

The Januária composite section (**Figure 4**) is composed of three minor sections, Cônego Marinho (CM), Barreiro (BAR) and Januária-Lontra (JL), all located at the North of Minas Gerais State, Brazil. Above the unconformity that separates the Bambuí Group from the basement, grey calcilutites (0–4 m) presenting aragonite pseudomorphs (cap carbonates) are overlapped by pink carbonates (4–19 m) that transition to light grey fine-grained carbonates (19–25 m) interleaved with pelitic siliciclastic layers. The presence of such layers was interpreted as evidence for a deep environment, therefore, at this interval, Caetano-Filho et al. (2019) set the maximum flood surface for the section. Overlying the light grey limestones, there are dark grey calcisiltites (25–58 m) intercalated with thin beds of clay. From 58 to 98 m, carbonates become gradually coarser and flat pebble breccias. At the top of the Sete Lagoas Formation, there are dolostones (98–100 m) with intraclasts and vugular porosity, which are interpreted as the result of a shallow to subaerial conditions (Caetano-Filho et al., 2019). Above them, an unconformity marks the end of the first second-order sequence. Following a gap of unknown thickness, the Serra de Santa Helena Fm. outcrops in a 20 m-thick succession of laminated to massive siltstones and mudstones and it is overlapped by the 20 m-thick package of limestones of the Lagoa do Jacaré Formation, which shows features such as oolites, intraclastic breccias and planar-parallel lamination. This section is detailed described in Caetano-Filho et al. (2019).

Arcos Section

The Arcos section (**Figure 5**) consists of two drillcores of about 200 m that were obtained by mining companies within the area of the city of Arcos, Minas Gerais, Brazil. Its detailed description can be found in Kuchenbecker et al. (2011, 2013) and will be summarized here. The basement comprises slightly deformed dark-green to grey granodiorites, above it, in an irregular contact, a 0.5 m-thick layer of the Carrancas diamictite occurs, containing clasts from the basement, besides clasts of limestones, siltite and quartz. The next 9 m of the section encompasses light-grey impure limestone intercalated with calcilutites. Microbial lamination is present so as fenestral porosity, commonly filled with sparry calcite and more rarely with crysptocrystalline silica. From 600 to 608 m, the terrigenous content diminishes and calcilutites are the dominant lithology and, occasionally, there is the occurrence of impure calcarenite. Stylolites and other dissolution structures are present, and at the top of this segment, there are aragonite pseudomorphs. Pyrite crystals, euhedric or framboidal, are also a common feature. Between 608 and 627 m the detrital content increases remarkably and the interval is marked by mudstones and siltstones, and, more rarely, by calcilutites. Such enhance in the detrital content was used as a guide to determine the maximum flood surface of the Arcos section (Caetano-Filho et al., 2019). Again, from 627 to 668 m, the terrigenous content is very low and limestones featuring microbial laminations predominate. However, from time to time, intraclastic calcarenites are also found. At the segment that goes from 668 to 705 m, calcilutite exhibiting microbial structures intercalates with black shaly rocks presenting a crinkled lamination. Then, until 718 m, calcilutites are the major lithology. From 718 to 738 m there are oolitic and intraclastic calcarenites. The interval between 738 and 761 m is heavily dolomitized, featuring oolitic and intraclastic doloarenites, sometimes laminated. The dolomitization is evidence of regression; therefore, at this interval, there is an unconformity that marks the end of the first second-order sequence and the beginning of the second second-order sequence. Following the dolomitic rocks, the Arcos section comprises, again, calcilutites with microbial structures, until the end of the section.

Well 1 Section

The Well 1 section (**Figure 6**) is a continuous drill core that was drilled in the southern São Francisco basin during hydrocarbon exploration campaigns. The detailed stratigraphy and depositional environment of Well 1 is present by Reis and Suss (2016). Its base, which will be investigated in this work, is approximately 430 m-thick, consisting of the thickest studied section presented here. An erosional unconformity marks the appearance of the Carrancas diamictite (muddy matrix sustaining

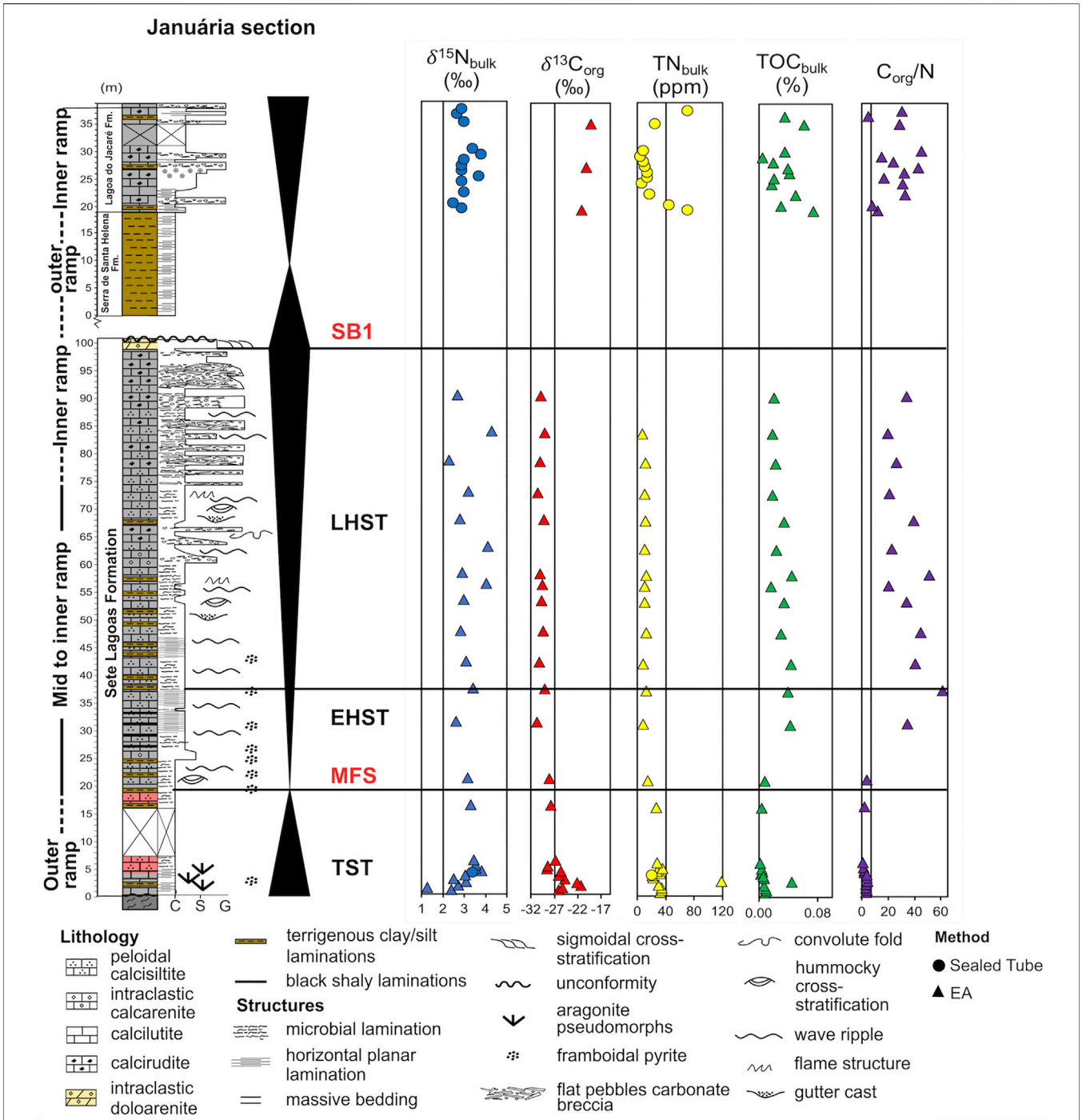

FIGURE 4 | Januária section: Depositional environments, lithologies, structures and sequence stratigraphy framework. $\delta^{15}N$ data was obtained in this study and $\delta^{13}C_{org}$ was published by Caetano-Filho et al. (2021). The axis on the C_{org}/N column is fixed on the Redfield ratio (6.6). System tracts: TST, Transgressive System Tract; MFS, Maximum Flooding Surface; EHST, Early Highstand System Tract; LHST, Late Highstand System Tract; SB1, Sequence Boundary. Granulometry scale: C, clay; S, sand; G, gravel. Adapted after Caetano-Filho et al. (2019).

clasts of metasedimentary rocks, granitoids and quartz veins) above the basement. The conglomerate grades upward to recrystallized dolomites ~80 m-thick) cemented by sparry dolomite and chert; wave ripples and hummocky stratification are present as well. From 1100 to 1075 m-depth dark shales intercalate with limestones, and from 1075 to 1045 m-depth a thick layer of shale containing pyrite closes this portion of the drill core. In the middle of this interval, the maximum flood surface was set (Caetano-Filho et al., 2019), as it represents deeper facies. Above the shaly interval, until approximately 880 m-depth,

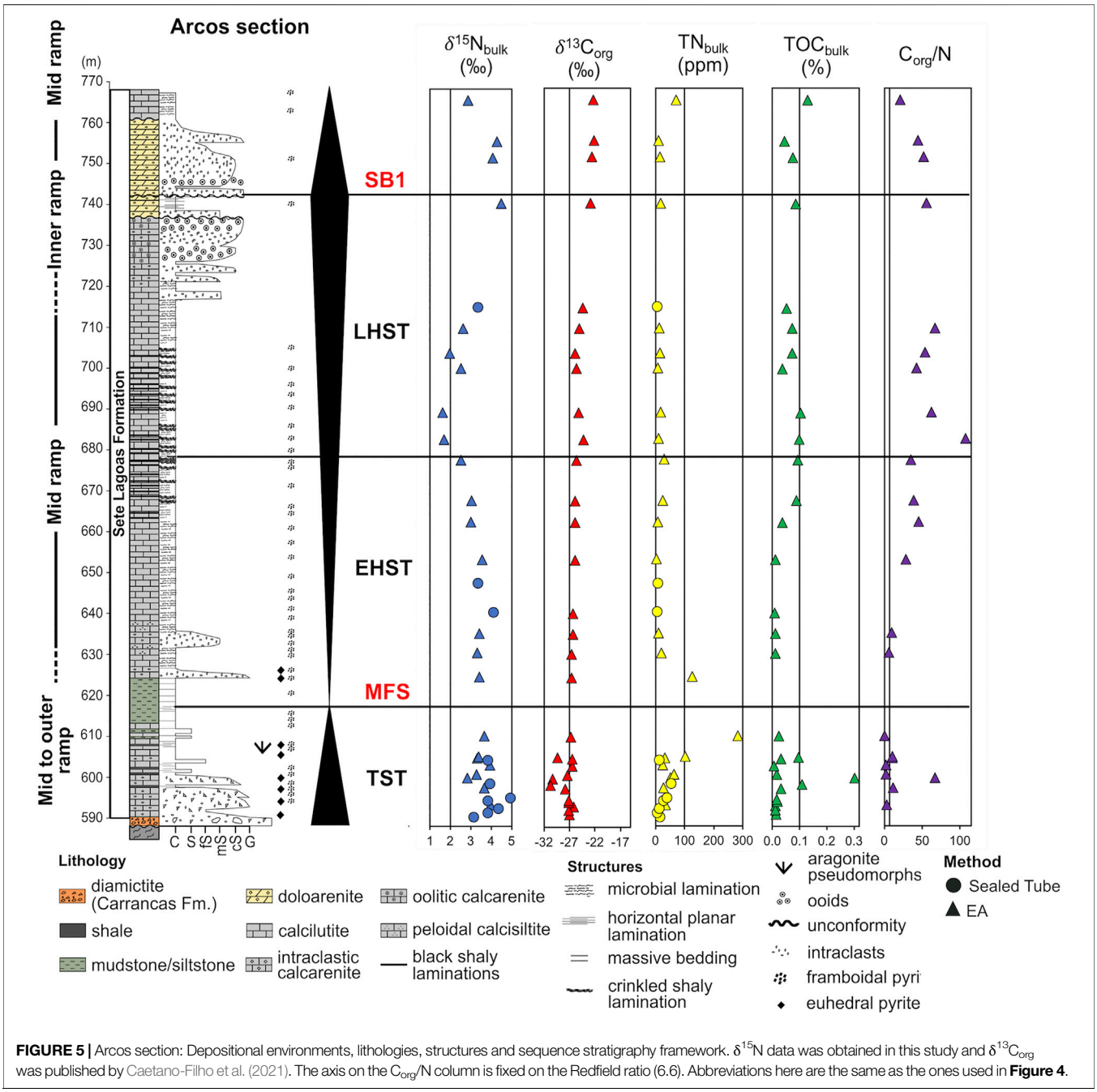

FIGURE 5 | Arcos section: Depositional environments, lithologies, structures and sequence stratigraphy framework. $\delta^{15}N$ data was obtained in this study and $\delta^{13}C_{org}$ was published by Caetano-Filho et al. (2021). The axis on the C_{org}/N column is fixed on the Redfield ratio (6.6). Abbreviations here are the same as the ones used in **Figure 4**.

greenish siltstones intercalate with calcilutites, calcarenites and calcirudites. Structures such as wavy, lisen and flaser beddings, wave ripples and hummocky stratification are reported. From 880 to 720 m-depth the section comprises dark-limestones of varied granulometry, in which wavy ripples, gutter casts, hummocky and horizontal planar lamination are described at the base of this segment and ooids, trough cross-bedding, planar cross-stratification and microbial lamination at the top. Also, associated with these microbial laminations, there is the limit of the first second-order sequence, an erosional surface at the base of peritidal channels limestones (Caetano-Filho et al., 2019).This is the only studied section in which there are no dolostones associated with the end of the first second-order sequence. The uppermost 30 m of Well 1 comprises shales with minor intercalations of calcirudites and calcarenites, pyrite is a common feature.

Preparation of the Samples for Analysis

In total, 177 samples were analysed, from these, 86 were from Well 1, 46 from Januária and 45 from Arcos. A stratigraphic resolution of 1 m was deployed for the cap carbonate interval, except Well 1, in which the resolution was 3 m. Also, for the

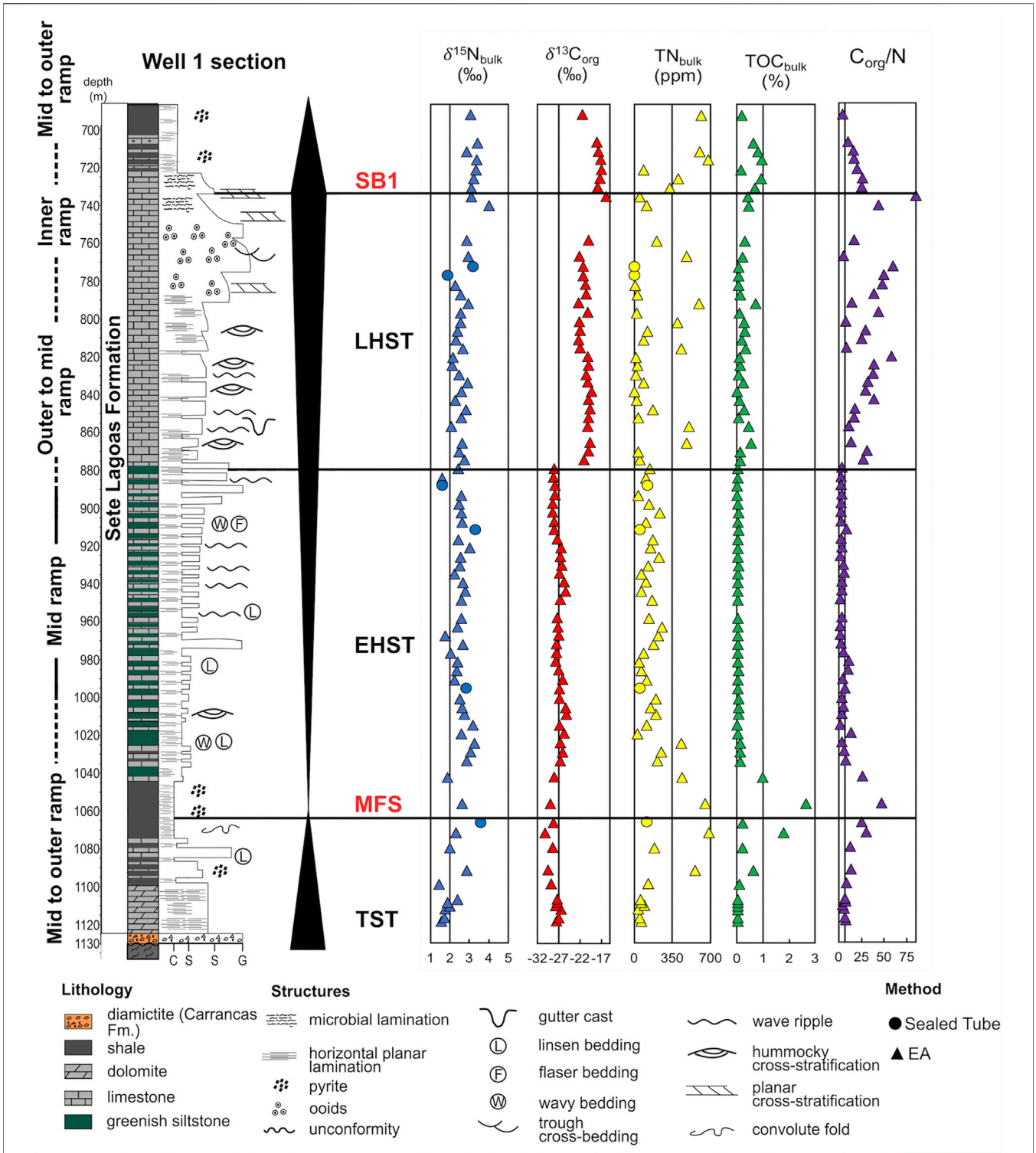

FIGURE 6 | Well 1 section: Depositional environments, lithologies, structures and sequence stratigraphy framework. $\delta^{15}N$ data was obtained in this study and $\delta^{13}C_{org}$ was published by Caetano-Filho et al. (2021). The axis on the C_{org}/N column is fixed on the Redfield ratio (6.6). Abbreviations here are the same as the ones used in **Figure 4**.

second sequence of the Januária section, the resolution of sampling was 1 m. For the rest of the sections, the interval was of 5 m, encompassing all the systems tract intervals defined by Caetano-Filho et al. (2019). To acquire $\delta^{15}N_{bulk}$ (N bounded to clays + N bounded to kerogen) data, the rocks were crushed into smaller pieces using mortar and pestle and were

subsequently pulverized using a tungsten carbide mill. The carbonate fraction was removed by adding 25 ml of 5 N HCl to 3–15 g of sample for 12 h at 25°C. The reaction proceeded after that at 80°C for 2 h. Leachate was centrifuged and discarded and the residue of this procedure was rinsed with distilled water until its pH was neutral and was then dried in an oven at 50°C. This allowed to concentrate N in the residue, a necessary step given the high carbonate content and very low TOC of most samples.

δ^{15}N, Total N and Total Carbon – Elemental Analyzer

To obtain the $\delta^{15}N_{bulk}$ data, samples were analyzed on an elemental analyser Thermo Scientific EA Flash 2000 coupled to a Thermo Scientific Delta V+, at Pôle de Spectométrie Océan, University of Western Brittany, France. For this, 5–10 mg of the insoluble residue of each sample was weighted in tin capsules and dropped by an autosampler into an oxidation furnace at 1020°C. An 8 s injection time of dioxygen at a flux of 240 ml/min was used to accomplish the flash combustion. To avoid incomplete oxidation of the flash combustion products, chromium(III) oxide and silver-plated cobalt oxide were added to the oxidation reactor. The produced gas was transported by continuous helium flow (100 ml/min) to a reducing column containing activated copper (heated at 650°C), which enabled the removal of oxygen in excess and the conversion of NO_x to N_2. Water vapor was removed from the gas using anhydrous magnesium perchlorate. The rest of the gases were separated using gas chromatography and were introduced into the mass spectrometer *via* a Thermo Scientific ConFlo IV universal interface. Total nitrogen (TN) was measured by the Thermal Conductivity Detector of the Flash EA 2000 and in this work, we report TN_{decarb} as the measured N concentration in the insoluble residue obtained after HCl leaching. $\delta^{15}N_{bulk}$ data is reported in per mil (‰) deviation from the atmospheric N isotopic composition ($\delta^{15}N_{air}$ = 0‰). The average uncertainty was calculated based on repeated measurements of the reference standard SED-IVA (sediment; + 4.42‰) and the in-house standard LIPG (yeast; −0.16‰) and it was better than 0.15‰ (2σ) for $\delta^{15}N_{bulk}$ and better than 0.03% (2σ) for N total concentration. This work also reports total nitrogen in samples (TN_{bulk}), which was calculated gravimetrically based on the amount of mass of sample remaining after the HCl leaching. Most of the total carbon data used here was published by Caetano-Filho et al. (2021), except for 11 samples from the second second-order sequence of Januária and one sample from Arcos that were measured at the Institut de Physique du Globe de Paris using a Flash EA 1112 coupled to a Thermo-Fisher Delta + XP isotope ratio mass spectrometer. The analytical procedure is similar to the one already described in Caetano-Filho et al. (2021) and the reproducibility of duplicate samples was better than 0.02% (2σ).

$\delta^{15}N_{bulk}$ and Total N – Sealed Tube Combustion + Dual Inlet Mass Spectrometer

For some of the samples from Arcos, Well 1 and Januária the nitrogen content was too low to obtain accurate results using the EA method. In these cases, when there was still enough material, samples were measured using what is known as the classical sealed tube method (Ader et al., 1998, 2016) at the Institut de Physique du Globe de Paris. In this method, the N_2 is extracted and purified using a vacuum line (Ader et al., 1998, 2016). For this purpose, quartz tubes were filled with previously purified CuO, Cu wires and sample. Then, the tubes were attached to the vacuum line and were degassed under 150°C until high vacuum conditions were obtained. Subsequently, the tubes were flame-sealed and proceeded to the combustion step, in which the tubes were heated in a furnace at 950°C for 6 h to allow the CuO to decompose into Cu and O, as the liberated O causes the combustion of the sample, which generates water, dinitrogen, carbon dioxide and nitrogen oxides as products. Then, the tubes are cooled down until 600°C for 2 h, to allow for the NO_x to react with Cu to generate N_2 and CuO. After the combustion, the generated gas was extracted and purified using the vacuum line. CO_2 and H_2O were separated from N_2 using a liquid nitrogen trap. After the purification step, the gas was concentrated and pushed into a sample vessel using a Toepler pump, which also allows the quantification of the extracted N_2. To assess possible contaminations coming from the vacuum line, blanks were commonly done, yielding less than 0.02 μmol of gas within the vacuum line system, which is negligible considering the amount of N_2 in Bambuí samples. The extracted gas was analyzed using a Thermo-Fisher Delta + XP mass spectrometer with a dual inlet introduction system to determine the nitrogen isotope composition. Nitrogen isotopes are measured in masses 28, 29 and 30 and masses 12 (C), 32 (O_2), 40 (Ar) and 44 (CO_2) are tracked to check for possible contaminations. The precision of $\delta^{15}N_{bulk}$ values was better than 0.5‰ (2σ), estimated from multiple measurements of a batch of samples. Accuracy was monitored by measuring certified materials IAEA-N1(+0.4 ± 0.2‰) and IAEA-N2 (+20.3 ± 0.2‰) and IPGP internal standard MS#5 (+14.9 ± 0.5‰).

K and Al Contents

K and Al contents were measured using a portable XRF device Thermo Scientific Niton XL3t provided by the Geological Survey of Brazil (CPRM). Sample slabs were polished and veins or terrigenous laminations were avoided during measurements. A blank (SiO_2) and a certified reference material (QC 180-673; Thermo) were run after every batch of 30 samples. The blanks present K content that was less than 0.01 ppm and the reproducibility of the standard was better than 0.2% (1σ). The Al blanks were lower than the detection limits and the reproducibility of standards was better than 0.5% (1σ). K and Al content are reported in percentage (%).

RESULTS

δ^{15}N and Total N

From the initial batch of 177 samples, we obtained 152 results. 39 from Januária section, 34 from Arcos section and 79 from Well 1 section (**Figures 4–6**). The results of the isotopic compositions of bulk nitrogen ($\delta^{15}N_{bulk}$), total nitrogen samples in residues (TN_{decarb}) and total nitrogen in bulk rock (TN_{bulk}) are shown

in **Supplementary Table S1**. The results were paired with total organic carbon in the insoluble residue (TOC_{decarb}), total carbon in bulk rock (TOC_{bulk}) and $\delta^{13}C_{org}$ data published by Caetano-Filho et al. (2021) except for 11 samples from the second sequence of Januária and one from Arcos, whose TOC_{decarb} and TOC_{bulk} were obtained in this work. C_{org}/N ratios were calculated from measured TOC_{decarb} and TN_{decarb} on an atomic basis and are also reported in **Supplementary Table S1**; **Figures 4–6**. $\delta^{15}N_{bulk}$ values are fairly constant on the three sections ranging from a minimum of +1.3‰ in Januária to a maximum of +5.0‰ in Arcos, with an average value of +2.9‰ (n = 152). TN_{bulk} (ppm) values are low in all sections, with an average value of 119.3 ppm (n = 152). In respect of C_{org}/N ratios, they range from 0.63, in Januária, to a maximum of 107.4, in Arcos, while the average value for the three sections is 20.3 (n = 152), which is above the Redfield Ratio (6.6) for C_{org}/N. Even if our average C_{org}/N value is low for Precambrian rocks, similar C_{org}/N ratios have been reported on the Ediacaran/Cambrian transition in China (Kikumoto et al., 2014). In all sections, the lowermost samples display a remarkable enrichment in N compared to the Redfield value and this enrichment ends near the transition to the LHST, except in Well 1, in which occasionally samples with low C_{org}/N are reported in the upper segments of the section (**Figures 4–6**; **Supplementary Table S1**).

Januária Section

Januária section samples average $\delta^{15}N_{bulk}$ is +3.1‰ (n = 39), ranging from +1.3 to +4.3‰ (**Figure 4**). In its TST interval, a pronounced positive $\delta^{15}N_{bulk}$ excursion from +1.2 to +3.8‰ occurs on the post-glacial carbonates of this section. In the EHST interval, Januária values form a plateau around +3.0‰, however, in the LHST interval, the $\delta^{15}N_{bulk}$ data of Januária oscillate between ~+2 and ~+4‰. Meanwhile, during the second second-order sequence, the average $\delta^{15}N_{bulk}$ of Januária is +3.0‰ (n = 13). Januária average TN_{bulk} and C_{org}/N is 29 ppm and 20 (n = 39), respectively. In Januária, the low C_{org}/N interval is present in its 13 lowermost samples, with an average C_{org}/N of 2.7, which corresponds to the cap carbonates and the upper limit of the EHST interval.

Arcos Section

Considering the three studied sections, Arcos has the heaviest N mean isotopic composition, +3.4‰ (n = 34) with $\delta^{15}N_{bulk}$ going from +1.6 to +5.0‰ (**Figure 5**). Some excursions are present along Arcos profile. The TST interval of this section presents a shift in which $\delta^{15}N_{bulk}$ values go from +3.2 to 5.0‰. In the EHST interval, $\delta^{15}N_{bulk}$ values are stable (~+3.0‰), but in the LHST interval they fall to a minimum of +1.6‰ near EHST/LHST boundary and then they return to +3.4‰. During the second second-order sequence, the $\delta^{15}N_{bulk}$ values of Arcos section rise and its mean value during this interval is +3.8‰ (n = 3). Arcos section average TN_{bulk} and C_{org}/N is 37 ppm and 31 (n = 34), respectively. Here, the low C_{org}/N interval ends earlier than in the other sections, in the middle of the EHST interval. One sample is an exception in this segment, with a C_{org}/N ratio of 67, which drives the mean value of this interval to 12. Without this sample, the average value for Arcos low C_{org}/N interval would be 8.

Well 1 Section

Well 1 section has the lowest $\delta^{15}N_{bulk}$ mean, +2.5‰ (n = 79), with N signatures going from +1.4 to +4.0‰ (**Figure 6**). In the TST interval, the cap carbonates from Well 1 present a little positive $\delta^{15}N_{bulk}$ shift going from +1.5 to +2.8‰ and during the EHST and LHST intervals, the $\delta^{15}N_{bulk}$ values of the Well 1 section are around a plateau of +2.5‰. In the second second-order sequence, $\delta^{15}N_{bulk}$ values rise and the average N isotopic composition is +3.2‰ (n = 6). Well 1 section is enriched in N when compared to the other two sections, with a TN_{bulk} of 198 ppm (n = 79). Also, TN_{bulk} concentrations increase as the amount of carbonate minerals diminish (**Supplementary Table S1**). This feature generated a remarkable zigzag pattern on the EHST interval of Well 1 section, in which limestones more or less rich in insoluble residue intercalates (**Figure 6**). In Well 1 the low C_{org}/N interval extends from the bottom of the section until the EHST/LHST boundary, except for values >6.6 that occurs near to the Maximum Flood surface (**Figure 5**) and rise the mean value of this interval to 7.

K and Al Contents

The average K content of samples is 0.4, 0.6 and 2.9%, whilst the average Al content is 1.0, 1.3 and 2.1% in Januária, Arcos and Well 1, respectively. Higher K and Al contents are reported during transgressive tracts, while the regressions show lower values (**Table 1**).

DISCUSSION

Preservation of $\delta^{15}N$ Primary Signals

We must evaluate the effects of diagenesis and metamorphism on the rock samples to check if the measured $\delta^{15}N_{bulk}$ values represent primary signals. In sedimentary rocks, N occurs mainly in two phases: within the organic fraction or present as clay-bound NH_4^+ substituting K^+ in crystal lattices (Müller, 1977; Greenfield, 1992), together, they compose the N_{bulk} reservoir. The clay-bound NH_4^+ comes mainly from the *in-situ* degradation of organic matter, although it can come from external fluid circulations (e.g. Schimmelmann et al., 2009). During the early diagenesis, as organic matter is degraded and N_{org} is liberated as NH_4^+ with minimum isotopic fractionation (Möbius, 2013), a pool of ammonium within the pore waters is generated. This NH_4^+, depending on the mineralogy, permeability and porosity of sediments (Stüeken et al., 2017), can either be fixed into clay minerals substituting K (Müller, 1977; Greenfield, 1992) without fractionation (Ader et al., 2016) or/and it can be oxidized into NO_2^-, NO_3^- and N_2, which depends on the O_2 concentrations of the environment. Since partial oxidation of NH_4^+ leads to isotopic fractionation, diagenetic effects on $\delta^{15}N_{bulk}$ are enhanced under oxic conditions, as it favors the instability of ammonium. Under anoxic environments, studies have shown that diagenetic effects increase primary $\delta^{15}N$ signal of bulk sediments by less than +1‰, while in oxic environments the increment can reach +4‰ (Altabet et al., 1999; Lehmann et al., 2002). Studies using Rare Earth Elements and iron speciation indicate that the bottom

TABLE 1 | Al and K content average values during the transgressions and regressions.

Section	Average K content – TST and 2nd-sequence (%)	Average K content - HST (%)	Average Al content – TST and 2nd-sequence (%)	Average Al content - HST (%)
Januária	0.4	0.3	1.1	0.6
Arcos	0.7	0.4	1.7	0.6
Well 1	4.6	0.7	2.9	1.9

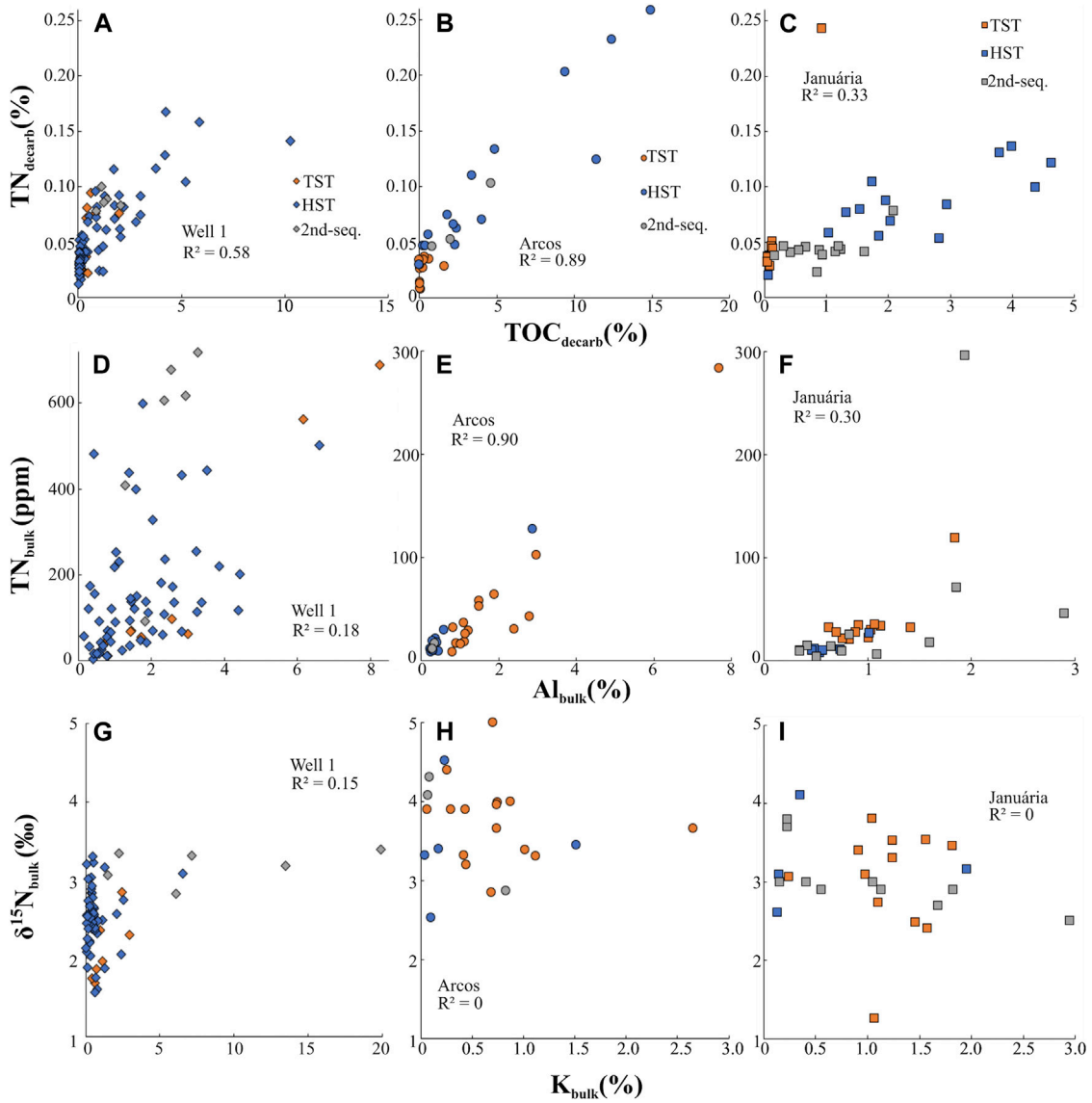

FIGURE 7 | Analyses of total nitrogen (TN), total organic carbon (TOC), Al, K and $\delta^{15}N$ in Well 1, Arcos and Januária sections.

waters of the Bambuí sea were anoxic in the intervals reported on this paper (Paula-Santos et al., 2018; Hippertt et al., 2019), which likely diminished the effects of diagenesis on the N isotopic signatures of the samples. Well 1 and Arcos section samples show a moderate and strong correlation (R^2 = 0.57 and 0.89, respectively) between TN_{decarb} and TOC_{decarb} (**Figures 7A,B**), indicating that N came mainly from the primary organic matter (Calvert, 2004). In Januária, the correlation is weaker, R^2 = 0.33 (**Figure 7C**), however, its coefficient of determination is influenced by an outlier heavily enriched in N. When the outlier

is removed, R^2 rises to 0.75. None of the trendlines of TN_{decarb} and TOC_{decarb} plots pass through the origin, which shows that a fraction of N in the samples is clay-bound. The presence of NH_4^+ linked to clay minerals is also notable when Al_{bulk} values are plotted against N_{bulk} concentrations. In Well 1 (**Figure 7D**) a correlation between these proxies is not seen during the HST interval, which drives its R^2 to 0.18, however, the correlation is clear during the TST and second-sequence interval of this section. In Arcos (**Figure 7E**) and Januária (**Figure 7F**), the correlation is also clear, with an R^2 of 0.90 and 0.30, respectively. The apparently low R^2 of Januária is caused by one N_{bulk}-rich sample present in its second second-order sequence. One remarkable feature in all sections is the C_{org}/N ratio at their base. The ratios are low when compared to the modern redfield ratio (6.6), which might indicate that the samples are enriched in N compared to the organic matter from which they were generated. This enrichment of N, when coupled to the fact that some N may be linked to clays and not to organic matter, must be investigated since the excess in N can be non-primary. Alternatively, excess of N can be a result of N preservation at the expense of C. If the first alternative is true, the samples cannot be used for paleoenvironmental reconstruction.

Metasomatic alteration can add non-primary NH_4^+ to the rocks and this could have happened in the sections, especially along intervals in which lithological heterogeneities facilitate fluid percolation, such as in the EHST interval of the Well 1 section. However, such external ammonium would have been preserved in clay minerals substituting K, and the lack of correlation between K_{bulk} and $\delta^{15}N$ in all three sections (**Figures 7G–I**) argues against such external N contamination. Therefore, the low C_{org}/N observed in the base of the sections was likely caused by exceptional preservation of N, which occurred due to the *in-situ* degradation of organic matter and releasement of NH_4^+ that was later trapped by clay-rich sediments while C was lost. Another evidence for this is that the Al_{bulk}/TOC_{bulk} ratios are higher in the low C_{org}/N intervals (**Table 2**). This ratio shows that clays are abundant when compared to organic matter, which creates favourable condition for the preservation of N in the form of NH_4^+. The conversion of N_{org} to mineralized NH_4^+ that is subsequently trapped into clays does not imply significant changes on the original primary $\delta^{15}N_{bulk}$ signal, especially under anoxic conditions. This hypothesis also is corroborated by the strong correlation observed between TOC_{decarb} and C_{org}/N ratios of the sections (**Figures 8A–C**) (Calvert, 2004), pointing that carbon loss is the major responsible for C_{org}/N variations. Such scenario requires a process that oxidizes C and preserves N, which can be achieved *via* microbial sulfate reduction, a plausible process considering the visual abundance of pyrite in the base of all sections decreasing towards the top of the basal sequence (Caetano-Filho et al., 2019). As sulfate cannot oxidize NH_4^+ under most conditions, NH_4^+ tends to accumulate in anoxic pore waters (Stüeken et al., 2016) and then it is trapped in clay minerals. Metamorphism effects on $\delta^{15}N$ signatures increase with metamorphic grade, as ^{14}N is preferentially volatilized (reviewed by Thomazo and Papineau, 2013; Ader et al., 2016). Fortunately, samples from the Bambuí Group are metamorphosed under greenschist facies and their signature was unlikely altered by more than 1‰ (Ader et al., 2016). A negative correlation between $\delta^{15}N$ and TN_{decarb} is also an indicator of metamorphic effects on $\delta^{15}N$ due to metamorphism, as during thermal alteration mainly ^{14}N is lost from the system, lowering N content and enhancing $\delta^{15}N$ primary signatures. Except for Arcos, which presents a moderate negative $\delta^{15}N$ and TN_{decarb} correlation (R^2 = 0.48; **Figure 8E**), the other sections do not present such a negative trend (**Figures 8D,F**). However, Arcos average $\delta^{15}N_{bulk}$ values (+3.4‰, n = 34) are similar to ones of Well 1 (+2.5‰, n = 79) and Januária (+3.1‰, n = 39), which discredits the hypothesis of heavy alteration of primary $\delta^{15}N$. Furthermore, the sections do not show relevant $\delta^{15}N$ and C_{org}/N correlations (**Figures 8G–I**), which would be expected if metamorphic alteration of N signals was relevant. Arcos shows a weak negative trend (R^2 = 0.34), the opposite expected for a metamorphism influence, as N is preferentially lost in higher temperatures when compared to C (Ader et al., 2006). Lastly, C_{org}/N ratios are mainly under 100, which is consistent with Proterozoic data with little $\delta^{15}N_{bulk}$ alteration (e.g, Beaumont and Robert, 1999; Chen et al., 2019). Hence, it is reasonable to consider that $\delta^{15}N_{bulk}$ of the Bambuí Group reflects mainly the primary signals of the organic matter and the data can be used for paleoenvironmental reconstructions.

TABLE 2 | Al_{bulk}/TOC ratios in low and high C_{org}/N ratios interval.

Section	Al_{bulk}/TOC_{bulk} in low C_{org}/N segments	Al_{bulk}/TOC_{bulk} in high C_{org}/N segments
Januária	~112	~17
Arcos	~46	~4
Well 1	~112	~17

The Nitrogen Biogeochemical Cycle in the Bambuí Sea

Increasing Oxygenation During the Deposition of the TST Interval

All the studied sections present a positive $\delta^{15}N_{bulk}$ excursion, from a minimum of +1‰ to a maximum +5‰, depending on the section, during the first transgression registered in the Bambuí Group (**Figure 9**). Two scenarios can generate $\delta^{15}N_{bulk}$ values comprehended between ~−2 and ~+1‰ (e.g., Casciotti, 2009; Quan et al., 2013; Sigman and Fripiat, 2019).

(i) assimilation of NO_3^- from an ocean where denitrification occurs only in the sediments. This would require a fully oxygenated water column to prevent the conversion of NO_3^- to N_2 while the former is transported/sunk.
(ii) biological N_2 fixation using Mo-based nitrogenase as a dominant path of the N cycle;

In the Bambuí Group, the reported low values on the TST interval (~+1‰) cannot be explained by a fully oxygenated ocean without denitrification on the water column. This scenario is not only unrealistic for the Precambrian (Canfield et al., 2010; Ader et al., 2016; Stüeken et al., 2016), it does not fit the published

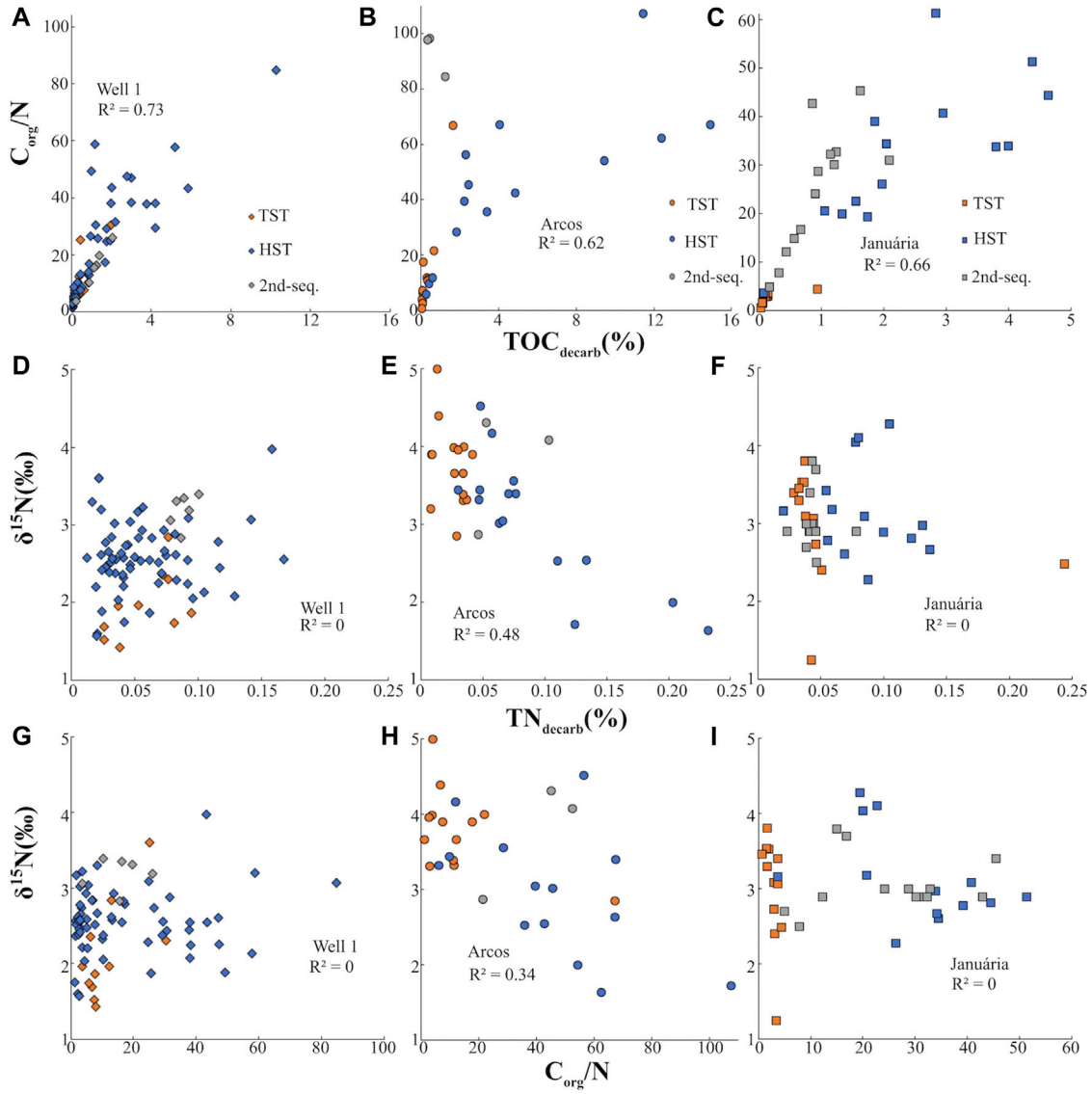

FIGURE 8 | Analyses of total nitrogen (TN), total organic carbon (TOC), C_{org}/N and $\delta^{15}N_{bulk}$ in Well 1, Arcos and Januária sections.

geochemical data available for the Bambuí which indicate bottom water anoxia (e.g. Caxito et al., 2018; Paula-Santos et al., 2018; Hippertt et al., 2019). Hence, the reported low $\delta^{15}N_{bulk}$ signature of Well 1 and Januária sections was likely caused by N_2 fixation using Mo-based nitrogenase in a redox stratified water body. The covalent bonds present in the N_2 molecule makes the conversion of N_2 to NH_3 energetically costly. Consequently, N_2 fixation requires more energy than NO_3^-/NH_4^+ direct assimilation to be processed (Alexander, 1984) and can only happen when no other form of N nutrient (NH_4^+ or NO_3^-) is available. As N_2 fixers are sensitive to O_2 (Gallon, 1981) anoxic conditions favours diazotroph and the presence of nutrient phosphorous (Tyrrell, 1999) and Mo (Seefeldt et al., 2009) are also important for the success of Mo-based N_2 fixation. Hence, $\delta^{15}N_{bulk}$ data points that at the beginning of the deposition of the cap carbonates from Well 1 and Januária sections (both presenting $\delta^{15}N_{bulk}$ values near +1‰ at their base) the water column was mainly anoxic which made N_2 fixation a main path of N-assimilation. NH_4^+ and NO_3^- would be near quantitatively consumed at the redoxcline by anammox and denitrification respectively. Phosphorus would also be in abundant supply as melting glaciers would deliver it to the Bambuí sea, however this hypothesis must be tested using other proxies. Besides that, as anoxic conditions enhance P residence time in the water column, environmental conditions prevented it from binding with Fe oxyhydroxides and being sequestered into sediments (Van Cappellen and Ingall, 1994). Finally, previous studies on the Bambuí Group show that Mo availability was high enough to support N_2 fixation (Hippertt et al., 2019). In fact, despite microbiological culture studies showing that low Mo-conditions might harm nitrogenase

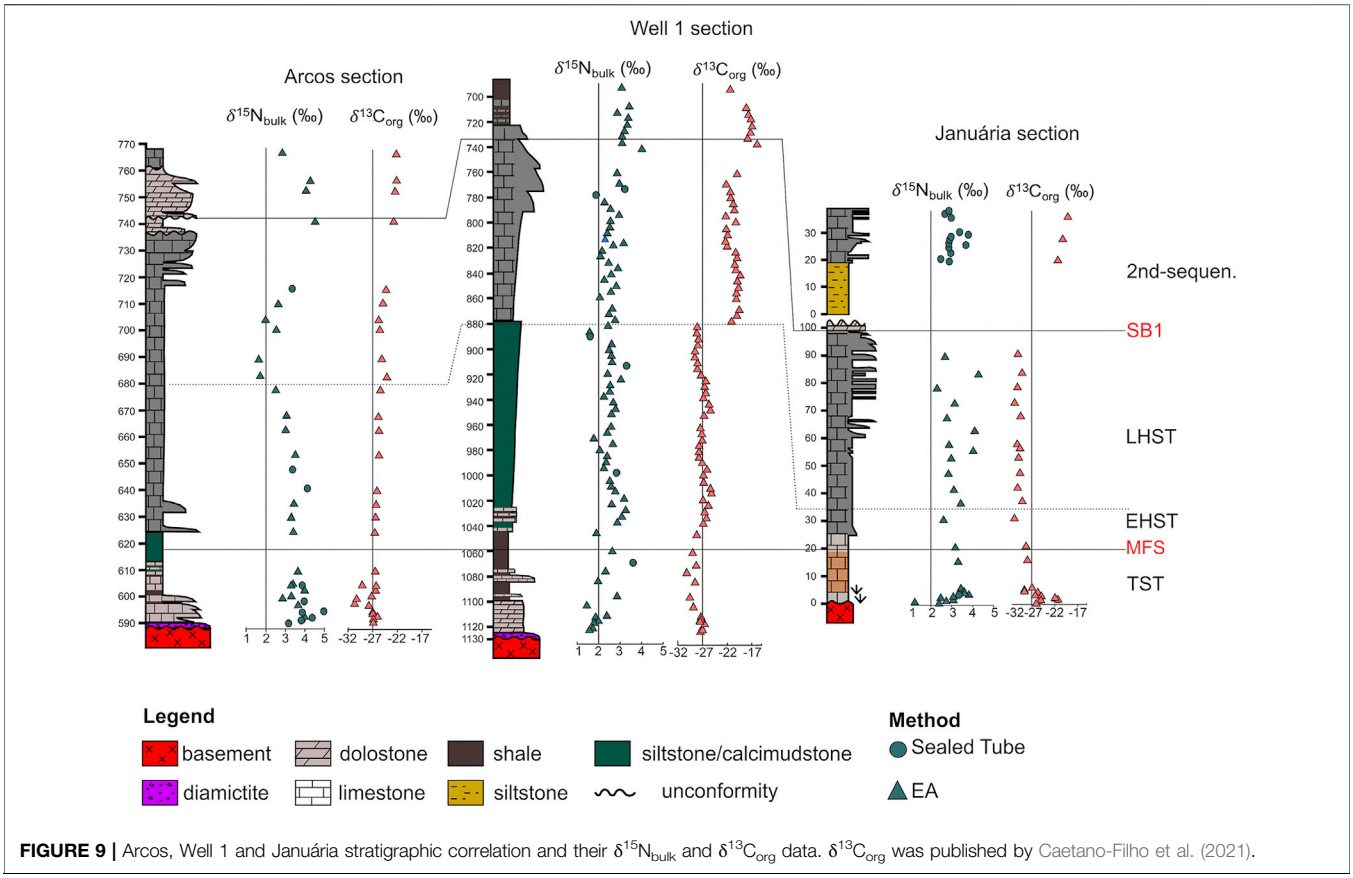

FIGURE 9 | Arcos, Well 1 and Januária stratigraphic correlation and their $\delta^{15}N_{bulk}$ and $\delta^{13}C_{org}$ data. $\delta^{13}C_{org}$ was published by Caetano-Filho et al. (2021).

enzyme operation (Zerkle, 2005), there is no evidence that Mo-scarcity played a role in diazotrophy activity in geological time (Stüeken et al., 2016).

As along the TST interval $\delta^{15}N_{bulk}$ values increase, another N-assimilation pathway must have competed with N_2 direct fixation. Two possibilities can be envisaged depending on redox state of the euphotic zone. In an anoxic photic zone (i.e. NH_4^+ is the main dissolved N species) $\delta^{15}N_{bulk}$ >+2‰ can be interpreted as:

(i) assimilation of NH_4^+ from a reservoir in which NH_3 dissociated from NH_4^+ and was volatilized (e.g. Stüeken et al., 2015);
(ii) non-quantitative assimilation of upwelled NH_4^+;
(iii) assimilation from an NH_4^+ pool that faced non-quantitative nitrification while the resultant nitrite and nitrate were completely reduced (e.g. Thomazo et al., 2011).

NH_4^+ can be dissociated to H^+ and volatile NH_3 and, as this reaction proceeds, ^{14}N-rich NH_3 is lost to the atmosphere and the remaining ammonium pool becomes strongly enriched in ^{15}N (Li et al., 2012). Thus, when this enriched NH_4^+ is assimilated, the sediments will yield very high $\delta^{15}N$ values. However, this process is observed only in highly alkaline lakes (pH > 9.25), which is not the case of Bambuí Group rocks (Li et al., 2012; Stüeken et al., 2015). The second alternative, non-quantitative assimilation of upwelled NH_4^+ is also unlikely. Microorganisms prefer to assimilate ^{14}N, which would generate more negative $\delta^{15}N$ values while enriching the residual NH_4^+ pool in ^{15}N. The absence of negative $\delta^{15}N$ values reported in any section is not in favour of this hypothesis. Finally, partial ammonium oxidation happens even when oxygen concentrations are in nanomolar levels (Füssel et al., 2012) and it is usually a quantitative reaction. Very few records of incomplete nitrification are reported on the geological history (Thomazo et al., 2011; Morales et al., 2014) and none of them for the Ediacaran/Cambrian, which discredit the third alternative. Moreover, all these paths involving NH_4^+ as the main nutrient are associated with big fractionation factors and should intuitively lead to significant stratigraphic $\delta^{15}N$ variability, which does not match the mild and consistent fractionation data reported on the Bambuí rocks. Hence, we assume in the following that samples from the TST interval which $\delta^{15}N_{bulk}$ values are higher than +2‰ do not reflect ammonium as a main nutrient.

In an oxidized photic zone (i.e. nitrate is stable), values of $\delta^{15}N_{bulk}$ >+2‰ is usually interpreted as:

(i) non-quantitative assimilation of NO_3^- (e.g. Sigman et al., 1999).
(ii) assimilation from a nitrate reservoir that experienced some degree of denitrification (e.g. Godfrey and Falkowski, 2009; Tesdal et al., 2013);
(iii) assimilation from a nitrate reservoir that experienced dissimilatory nitrate reduction (DNRA) (e.g. An and Gardner, 2002; Dong et al., 2011; Jensen et al., 2011);

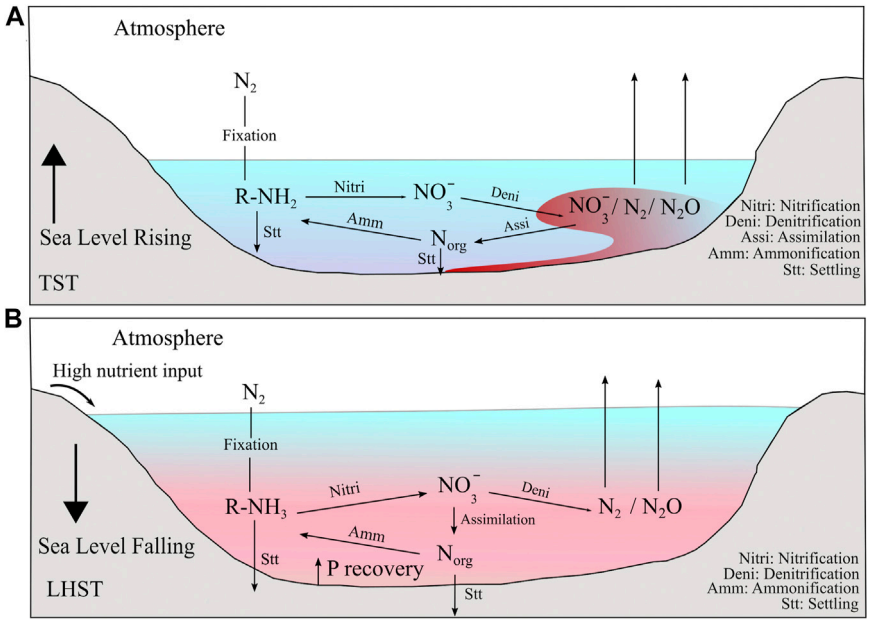

FIGURE 10 | Possible scenario of the N-cycle on the Bambuí Basin during the deposition of its basal sequences. **(A)** During the TST, a stable nitrate pool was established and the most dominant form of N available was nitrate that went through partial denitrification on zones of low oxygenation. **(B)** During the LHST, the high input of nutrients coming from the continent and P recovery under anoxic bottom water conditions, caused the limitation of NO_3^- in superficial waters, making N_2 fixation the main form of N acquisition by phytoplankton.

In the Bambuí, non-quantitative assimilation of upwelled NO_3^- is improbable. This alternative would require a large reservoir of nitrate to have built on deep oxygenated waters, which is not the case. Therefore, it is likely that $\delta^{15}N_{bulk}$ >+2‰ reported on TST interval is linked to the assimilation of a NO_3^- reservoir that faced dissimilatory nitrate reduction and/or denitrification. However, in DNRA, differently from denitrification, N does not escape from the water column, but it is converted to light bioavailable NH_4^+. Hence, if DNRA was a main path, one would expect to find in other samples a complementary light reservoir opposing the enriched $\delta^{15}N_{bulk}$ reported here. As the light reservoir was not found in any section, the importance of DNRA was likely minimal. Hence, discarded all others possibilities, the positive $\delta^{15}N_{bulk}$ excursion reported at the basal Januária and Well 1 section represents a shallow sea that was initially dominated by Mo-based N_2 fixation and later was enough oxygenated to support nitrate accumulation and assimilation from a pool that faced denitrification (Sigman and Fripiat, 2019) (**Figure 10A**). The built-up of a nitrate reservoir in the oxygenated surface waters during the transgressive tract on the euphotic zone matches geochemical data that suggests progressive oxygenation of the Bambuí seawater associated with the input of oxygenated freshwater. For instance, positively fractionated $\delta^{53}Cr$ (Caxito et al., 2018), punctual negative Ce anomalies (Caxito et al., 2018; Hippertt et al., 2019; Paula-Santos et al., 2020) and iron speciation/redox-sensitive elements data indicating locally oxygenated conditions (Hippertt et al., 2019) are reported in this interval. Importantly, in Januária and Well 1, $\delta^{15}N_{bulk}$ values associated with nitrate assimilation are low (maximum value of +3.8‰ in Januária) when compared to the mean value of modern nitrate (~+5‰, Tesdal et al., 2013). This implies that N_2 fixation was still playing an important role in bioproduction and also that the nitrate reservoir was small and denitrification occurred nearly quantitatively, i.e., with a reduced isotope fractionation at a shallow redoxcline. The lowermost sample from the Arcos section presents a $\delta^{15}N_{bulk}$ value of +3.2‰, which means that at the beginning of the transgression there was already a nitrate reservoir in this part of the basin. Moreover, Arcos' values rise to 5‰, implying reduced N_2 fixation and a large nitrate reservoir compared to the other sites. This points to more oxygenated surface waters in the South of the São Francisco basin paleohighs (Arcos section), compared to the forebulge grabens area (Well 1 section). Oxygenation in Arcos TST interval was also observed by Paula-Santos et al. (2020) using Ce anomalies.

Increasing Anoxia During the Highstand System Tract Interval

In the EHST interval, the $\delta^{15}N_{bulk}$ data point to a stable N-cycle, as no significant shift is N isotopic signature is observed in any of the sections (**Figure 9**). The $\delta^{15}N_{bulk}$ average values for the EHST are +2.9, +3.3 and +2.5‰ in Januária, Arcos and Well 1, respectively, suggesting the maintenance of the nitrate reservoir established in surface waters during the TST interval. Also, REY data shows that freshwater input was still happening during the EHST (Paula-Santos et al., 2020) deposition, which might have contributed to the maintenance of nitrate on surface waters. However, oxygenation was not pervasive, as $\delta^{15}N_{bulk}$ values are still low when compared to the modern nitrate reservoir, pointing to a shallow redoxcline and nitrate loss

compensated by N_2 Mo-based fixation. The $\delta^{15}N_{bulk}$ values from Arcos and Januária sections are slightly higher than in Well 1, indicating that surface waters were more oxygenated in shallow domains than in forebulge grabens.

In the LHST interval, the sections present different trends. Many geochemical proxies mark significant paleoenvironmental changes in this interval that are linked to the progressive restriction of this unit (e.g. Paula-Santos and Babinski, 2018; Paula-Santos et al., 2020). The LHST may also record a period of higher bioproductivity, a hypothesis that is further corroborated by its slightly higher TOC when compared to the other system tracts (**Figures 4–6**; Caetano-Filho et al., 2021). This could have been induced by a change to more congruent weathering regimes at the surrounding orogenic fronts that led to higher total alkalinity of seawater during the LHST (Paula-Santos et al., 2020), although proxies to quantify weathering fluxes are still required. These environmental changes are also tracked by N data. A negative excursion is present at the lower Arcos LHST and sometimes its $\delta^{15}N_{bulk}$ values are within the N_2 fixation range (<+2‰). As in the TST interval, there is no evidence that ammonium incomplete assimilation was a main path during the LHST, as the reported fractionation values are mild and constant, differently from large fractionations usually associated with NH_4^+ assimilation (e.g. Thomazo et al., 2011; Stüeken et al., 2015). Therefore the negative shift at the transition from the EHST to the LHST in Arcos section could be caused either by *1*) excess of nitrate and its incomplete assimilation or *2*) exhaustion of the nitrate reservoir forcing microorganisms to fix N. The first alternative is unlikely. In modern oceans, excess of nitrate is only achieved in zones named high-nutrient, low chlorophyll (HNLC) zones, where despite the abundance of macronutrients, the phytoplankton biomass is low, due to a shortage of iron, which seems not to occur in the Bambuí (Hippertt et al., 2019). Also, HNLC conditions are usually met in open oceans, a different scenario from the restricted Bambuí sea during the LHST (Edwards et al., 2004). Then, the drop in the $\delta^{15}N_{bulk}$ values during Arcos EHST/LHST transition is probably an effect of enhanced bioproductivity, as the nitrate reservoir that was built during the EHST was not able to support the high productivity related to high input of nutrients. In this scenario, the input of P due to the enhanced weathering disturbed the normal 16:1 ratio of $[NO_3^-]$:$[PO_4^{3-}]$ on seawater. Consequently, diazotrophic activity rose to restore this ratio (Tyrrell, 1999), which is reflected by low $\delta^{15}N_{bulk}$ values (**Figure 10B**). Also, at this stage, not only the input of phosphorus *via* weathering was high, but progressively anoxic conditions also favored the recycling of this nutrient (Van Cappellen and Ingall, 1994; Ingall and Jahnke, 1997), making it abundant when compared to nitrate. In addition to that, the restriction likely disturbed the circulation patterns of the basin, diminishing the amount of NH_4^+ that is upwelled and nitrified, making the supply of NO_3^- even shorter. As the availability of NO_3^- diminished, the energetic costly N_2 fixation became the main path to acquire N. High productivity associated to high N_2 fixation rates was also observed in modern environments, such as the Black Sea (Quan et al., 2013) and the Cariaco Basin (Haug et al., 1998). Importantly, as the Bambuí, these two settings are also restricted. Up section, in the LHST, the $\delta^{15}N_{bulk}$ values from Arcos rises from +1.6 to +3.4‰, implying that the nitrate reservoir was re-established, but it does not reach the +5.0‰ values reported in the TST interval. In Januária, there is not an abrupt shift in $\delta^{15}N_{bulk}$ during the transition from the EHST to the LHST interval as in Arcos. However, when one observes the $\delta^{15}N_{bulk}$ profile of the LHST interval in the Januária section, the most striking feature are the rapid changes of $\delta^{15}N_{bulk}$, as sometimes they interchange between values around +2.5 and +4.0‰, which creates a zigzag pattern (**Figure 4**). These increased variability indicate that in the central part of the São Francisco Basin shallow domains also faced instability of a limited superficial nitrate pool during regression, which was compensated by N_2 fixation. Also, the average $\delta^{15}N_{bulk}$ of the LHST from Januária (+3.2‰, $n = 12$) and Arcos (+3.3‰, $n = 9$) is low, which means that even when redox conditions permitted the stability of NO_3^-, the pool was not large and $\delta^{15}N_{bulk}$ still reflects a mix between N_2 fixation and NO_3^- assimilation. It is important to access that the fossil *Cloudina* sp. was reported (Warren et al., 2014) in this section and it is associated to the LHST interval (Caetano-Filho et al., 2019). The $\delta^{15}N_{bulk}$ values show that even if deep waters were anoxic (Hippertt et al., 2019), superficial waters could intermittently sustain a small nitrate reservoir, which is important given the fact that major *Cloudina* sp. reports are found in oxic contexts (Bowyer et al., 2017). The record of the LHST from Well 1 section differs from the other two, as no shift in the $\delta^{15}N_{bulk}$ values is observed in comparison to the EHST interval. The values reported for Well 1 section in the entire HST are low, nearly at the boundary of N_2 fixation and NO_3^- assimilation. The stability of $\delta^{15}N_{bulk}$ during the regression stages points that progressive restriction and relative changes in accommodation and sediment supply did not influence the N cycle in the forebulge graben setting compared with shallower domains. It also implies that during the regression stage, local controls affected the nitrogen cycle in the forebulge grabens, despite changes in sea level. One of those controls may have been poor wind mixing effects inside the extensional depocenters, which would have prevented the vertical mixing of superficial waters and enhance stratification in deep environments (Yang et al., 2018). Also, if the rates of sinking organic matter are low, this can move the redoxcline to shallower depths (Meyer et al., 2016). The TOC_{bulk} content of Well 1 during the HST is three times higher than the ones from Januária and Arcos section for the same interval, which suggests that bioproduction could be one of the local factors that caused consistent low values of $\delta^{15}N_{bulk}$. Finally, if we consider that the chemocline was at the same level in all the Bambuí sea, Well 1 would have a larger anoxic water column than the other two sections (**Figure 11**), which might have contributed to its consistent low values. In the LHST interval, the Bambuí was physically restricted and circulation was very inefficient. Therefore, the bioavailable NO_3^- recharge of surface waters was limited to diffusion from deeper waters or by induced water column mixing caused by storms (Ader et al., 2016). There are evidences of storms in Arcos and Well 1 LHST interval (Hummocky Cross-stratification, **Figures 5**, **6**), which explains why the $\delta^{15}N_{bulk}$ values are not entirely within the N_2-fixation range. However, such storms are occasional events and the NO_3^- reservoir was small. The scarcity of NO_3^- during the LHST is also corroborated by episodes of euxinia observed during this interval (Hippertt et al., 2019). Nitrate and sustained euxinia can never coexist because

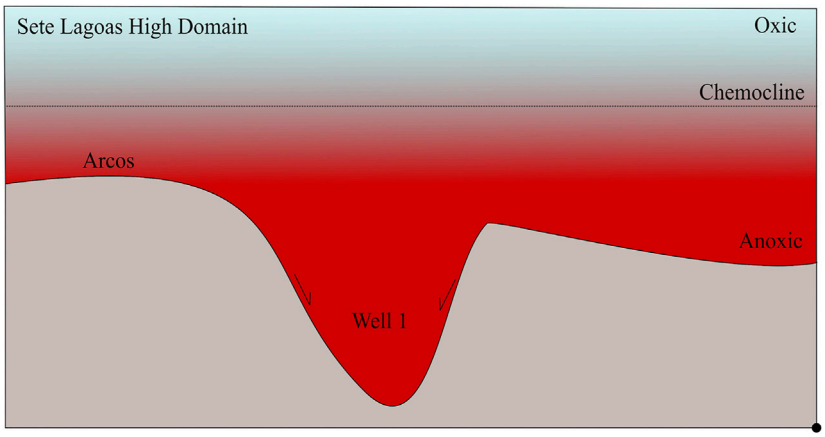

FIGURE 11 | Schematic representation of the Sete Lagoas High Domain. Well 1 is located inside a forebulge graben and Arcos in a shallower part of the Sete Lagoas Domain. Hence, if we consider that the chemocline was at the same level, Well 1 had a deeper anoxic water column than Arcos.

denitrification produce more free energy per mole of carbon than microbial sulfate reduction (MSR), being therefore a preferred respiratory pathway when SO_4^{2-} and NO_3^- coexist. For that reason, nitrate concentrations exert a primary role in the rates of MSR and this mechanism is prohibited when NO_3^- is available (Canfield, 2006). However, a form of N acquisition is essential to fuel the production of the organic matter that will be respired by MSR and consequently generate an H_2S pool. As this species cannot be NO_3^-, Boyle et al. (2013) argued that intermediate euxinic waters must be coupled to superficial waters in which the main path of the N-cycle is direct N_2 fixation, which is a plausible scenario in the Bambuí Group geological context.

Oxygenated Euphotic Zone During the Second second-Order Sequence

The sedimentary rocks from the second second-order sequence of the Bambuí Group are considered to be deposited under a fully restricted sea and this interval is marked by very high $\delta^{13}C_{org}$ values interpreted to be caused by high methanogenic activity under anoxic conditions (Caetano-Filho et al., 2021) and/or recycling of ancient carbonate platforms, higher burial rate of authigenic carbonate, and low-sulfate conditions (Uhlein et al., 2019; Cui et al., 2020). When one compares the $\delta^{15}N_{bulk}$ and the $\delta^{13}C_{org}$ data of the Bambuí during the second second-order sequence it is clear that they are decoupled, which shows that despite big changes in the carbon cycle, the nitrogen cycle was not much affected (**Figure 9**). Still, minor changes occurred. The $\delta^{15}N_{bulk}$ data from this sequence suggests that a nitrate pool was buildup, although smaller and not stable as the one from the basal TST interval, which implies that at least superficial waters were oxygenated. Furthermore, samples from this interval do not present a consistent REY pattern, which shows that freshwater input might have happened during its deposition (Paula-Santos et al., 2020), influencing superficial oxygenation. In all sections, in the second second-order sequence $\delta^{15}N_{bulk}$ values are around ~+3‰. Even in Well 1 section, whose $\delta^{15}N_{bulk}$ data were stable during the EHST/LHST, $\delta^{15}N_{bulk}$ values rise during the second transgression. Since values of $\delta^{15}N_{bulk}$ higher than +2.0‰ can be interpreted as assimilation from a nitrate pool that went through partial denitrification, $\delta^{15}N_{bulk}$ values suggest that during the second second-order sequence transgression there was more oxygen dissolved in superficial waters of forebulge grabens than during the EHST/LHST. As both transgressions recorded in the Bambuí basal second-order sequences present a rise in $\delta^{15}N_{bulk}$ values, which contrast with the regressive tract data, one must think if there is a relationship between transgression and oxygenation. In fact, it was suggested that in the Ediacaran Nama Group persistent oxygenation in mid-ramp settings was controlled by basin hydrodynamics, as data from this unit implies that ventilation was favored by highly energetical flooding events (Wood et al., 2015). Although the tectonic setting of the Bambuí (restricted epicontinental sea) and Nama groups (open sea connected to global ocean) are different, the data presented here show that sea-level changes affected oxygenation and the N-cycle of the former. However, the nitrate pool of the second transgression was not as stable or large as the one from the first TST, which can be inferred by their lower values and also $\delta^{15}N_{bulk}$ oscillation, especially in Arcos section. This is probably a response to a heavily stratified water column, as proposed by other studies (Hippertt et al., 2019; Caetano-Filho et al., 2021).

The Nitrogen Cycle and its Implications for Life Systems

The metazoan fossil record of the Bambuí Group is scarce when compared to other geological Ediacaran/Cambrian units (e.g. Nama Group, Doushantuo Formation). It was hypothesized that such scarcity could be related to anoxia, euxinia, hypersaline and methane-rich conditions of the Bambuí seawater (Hippertt et al., 2019; Caetano-Filho et al., 2021). In addition to this, $\delta^{15}N_{bulk}$ points out that as expected in such a situation, the N-cycle (and hence redox conditions) functioned with a reduced nitrate pool, which could have contributed to hinder the sustainability of complex forms of life. The link between

oxygenation and the Cambrian explosion has been discussed for more than 60 yr (e.g., Nursall, 1959; Wood et al., 2020). Metazoans can indeed habit environments with low oxygen concentrations and some studies even suggest that the amount of O_2 necessary for their metabolism was achieved much earlier than the first appearance of animals on the fossil record (e.g., Mills et al., 2014). However, poorly oxygenated environments cannot support complex life systems or large organisms (Sperling et al., 2013), and concordantly, most of the Ediacaran/Cambrian Fauna is recorded at oxygenated habitats, even if oxygenation was transient (Bowyer et al., 2017; Wood et al., 2019). Therefore, the fluctuations of the generally shallow chemocline's depth in the Bambuí basin may have been one of the drivers of its low macrofauna diversity. In fact, the metazoans reported at the Bambuí Group were found on the Januária's LHST interval, which is, if $\delta^{15}N_{bulk}$ values are considered, the most nitrate rich and oxygenated site during this stage, although with a strong variability, indicating that conditions were unstable (*see* **section 5.2.2**). Redox conditions control the availability of nitrate, which is the form of nitrogen preferred by eukaryotes, as they cannot process direct N_2 fixation and other forms of fixed-N, such as NH_4^+, are mainly consumed by prokaryotes (Fawcett et al., 2011). Complex and large-celled phytoplankton communities generate food webs that are more effective to transfer nutrients and energy to higher trophic levels (Irwin et al., 2006) and the rise of eukaryotes is linked to the development of metazoans as they have higher energetic demands (Brocks et al., 2017). As the $\delta^{15}N_{bulk}$ values from Bambuí Group suggest that nitrate pools were not large or stable, especially during regressions, this could have affected the large-celled plankton and consequently metazoans. In addition, if a large eukaryote community do not develop and the phytoplankton is dominated by prokaryotes, due to their low mass, the sinking rate of the organic matter particulates is low and remineralization of this organic matter is faster and occurs within the water column, enhancing anoxia (Lenton et al., 2014). The relation between nitrate and complex life forms during the Ediacaran/Cambrian transition has been studied mainly in South China (e.g., Wang et al., 2018; Xiang et al., 2018; Liu et al., 2020; Xu et al., 2020) and although it is not possible to link the Bambuí Group to global trends, due to its marine isolation, this study brings more data to clarify how the N-cycle operated at that time. These episodes of nitrate limitation reported here are probably one of the many factors that might have driven the inhospitality of the Bambuí sea, associated with phases of methane or free H_2S in the water column (Caetano-Filho et al., 2021).

CONCLUSION

Relative sea-level variations seem to exert control in the Bambuí N-Cycle. During the first transgression interval (TST), in all the studied sections $\delta^{15}N_{bulk}$ values rise from a minimum of ~+1.0‰ to a maximum of ~+5.0‰, which is parsimoniously explained as a rise of the nitrate reservoir and hence oxygen levels in surface waters. As the restriction of the Bambuí increases (LHST) the NO_3^- stability is disturbed, which is shown by a negative excursion observed in the transition of Arcos EHST to LHST and by increased variability in the $\delta^{15}N_{bulk}$ values of Januária. The low $\delta^{15}N_{bulk}$ observed in the LHST interval of both sections is interpreted as the result of N_2 fixation using Mo as cofactor, indicating a small NO_3^- reservoir. Finally, the slightly higher $\delta^{15}N_{bulk}$ values of the second second-order transgressions show that the nitrate pool increased again, but not to the level that prevailed during the first transgression. In this latter interval, N_2 fixation still played a significant role, maybe due to the restriction of the Bambuí seawater at this stage. Hence, the $\delta^{15}N_{bulk}$ data shows that the basin operated in periods in which N_2 fixation and NO_3^- assimilation intercalated as the dominant path of nitrogen assimilation by primary producers, which can be interpreted in terms of more or less oxygen within superficial waters. Nitrate is a very important nutrient for eukaryotes primary producers and eukaryotes are necessary to fuel higher trophic levels, its depletion in some intervals might be one of the factors that drove the hostile conditions for metazoans in the Bambuí seawater.

DATA AVAILABILITY STATEMENT

The raw data supporting the conclusions of this article will be made available by the authors, without undue reservation.

AUTHOR CONTRIBUTIONS

PF-F analyzed the nitrogen isotopic composition of the samples, interpreted the data and wrote the manuscript. SC-F, MA, PS, and VR acquired N data. SC-F, GP-S, CG, and CB-R obtained K and Al data and also did fieldwork. MB, MK, HR, and RT assisted with tectonic, stratigraphic, petrographic, geochemical information regarding the Bambuí Group and also with the conceptualization of this project. MK and HR provided samples from the sections of Arcos and Well 1 respectively. All the authors collaborated on the final version of the manuscript and assisted with geological interpretations.

FUNDING

This study was funded by the São Paulo Research Foundation (FAPESP) thematic project The Neoproterozoic Earth System and the rise of biological complexity grant 2016/06114-6. PF-F holds a FAPESP scholarship grant #2019/13228-6.

ACKNOWLEDGMENTS

We acknowledge to Lhoist and Petra Energia S.A. for providing drill core samples, Brazilian Geological Service (CPRM) for providing the XRF device, CAPES for institutional support and Pôle de Spectométrie Océan and Institut de Physique du Globe de Paris staff for the technical support in data acquisition. PF-F holds a FAPESP scholarship grant #2019/13228-6. MB, RT, and MK are

fellows of the Brazilian Research Council (#307563/2013-8, #206997/2014-0 and #309106/2017-6, respectively). We are also thankful to the reviewers Dr. Xinqiang Wang and Dr. Fabricio Caxito for constructive suggestions, and to Dr. Graham Shields for the editorial handling of the manuscript.

SUPPLEMENTARY MATERIAL

The Supplementary Material for this article can be found online at: https://www.frontiersin.org/articles/10.3389/feart.2021.692895/full#supplementary-material

REFERENCES

Ader, M., Boudou, J.-P., Javoy, M., Goffe, B., and Daniels, E. (1998). Isotope Study on Organic Nitrogen of Westphalian Anthracites from the Western Middle Field of Pennsylvania (U.S.A.) and from the Bramsche Massif (Germany). *Org. Geochem.* 29, 315–323. doi:10.1016/S0146-6380(98)00072-2

Ader, M., Cartigny, P., Boudou, J.-P., Oh, J.-H., Petit, E., and Javoy, M. (2006). Nitrogen Isotopic Evolution of Carbonaceous Matter During Metamorphism: Methodology and Preliminary Results. *Chem. Geology.* 232, 152–169. doi:10.1016/j.chemgeo.2006.02.019

Ader, M., Sansjofre, P., Halverson, G. P., Busigny, V., Trindade, R. I. F., Kunzmann, M., et al. (2014). Ocean Redox Structure Across the Late Neoproterozoic Oxygenation Event: A Nitrogen Isotope Perspective. *Earth Planet. Sci. Lett.* 396, 1–13. doi:10.1016/j.epsl.2014.03.042

Ader, M., Thomazo, C., Sansjofre, P., Busigny, V., Papineau, D., Laffont, R., et al. (2016). Interpretation of the Nitrogen Isotopic Composition of Precambrian Sedimentary Rocks: Assumptions and Perspectives. *Chem. Geology.* 429, 93–110. doi:10.1016/j.chemgeo.2016.02.010

Alexander, M. (1984). *Biological Nitrogen Fixation: Ecology, Technology and Physiology*. Boston, MA: Springer, 1–258. Available at: https://doi.org/10.1007/978-1-4613-2747-9 (Accessed May 22, 2020).

Alkmim, F. F., and Martins-Neto, M. (2001). "Bacia Intracratônica Do São Francisco: Arcabouço Estrutural e Cenários Evolutivos," in *Bacia do São Francisco: Geologia e Recursos Naturais*. Editors C. P. Pinto and M. Martins-Neto (Belo Horizonte: SBG/MG).

Alkmim, F. F., and Martins-Neto, M. A. (2012). Proterozoic First-Order Sedimentary Sequences of the São Francisco Craton, Eastern Brazil. *Mar. Pet. Geology.* 33, 127–139. doi:10.1016/j.marpetgeo.2011.08.011

Altabet, M. A., Pilskaln, C., Thunell, R., Pride, C., Sigman, D., Chavez, F., et al. (1999). The Nitrogen Isotope Biogeochemistry of Sinking Particles from the Margin of the Eastern North Pacific. *Deep Sea Res. Oceanographic Res. Pap.* 46, 655–679. doi:10.1016/S0967-0637(98)00084-3

An, S., and Gardner, W. (2002). Dissimilatory Nitrate Reduction to Ammonium (DNRA) as a Nitrogen Link, Versus Denitrification as a Sink in a Shallow Estuary (Laguna Madre/Baffin Bay, Texas). *Mar. Ecol. Prog. Ser.* 237, 41–50. doi:10.3354/meps237041

Babinski, M., Vieira, L. C., and Trindade, R. I. F. (2007). Direct Dating of the Sete Lagoas Cap Carbonate (Bambuí Group, Brazil) and Implications for the Neoproterozoic Glacial Events. *Terra Nova* 19, 401–406. doi:10.1111/j.1365-3121.2007.00764.x

Barbosa, O., Braun, O. P. G., Dyer, R. C., and Cunha, C. A. B. M. (1970). *Geologia da região do Triângulo Mineiro*. Rio de Janeiro: DNPM/CPRM.

Beaumont, V., and Robert, F. (1999). Nitrogen Isotope Ratios of Kerogens in Precambrian Cherts: A Record of the Evolution of Atmosphere Chemistry? *Precambrian Res.* 96, 63–82. doi:10.1016/S0301-9268(99)00005-4

Bowyer, F., Wood, R. A., and Poulton, S. W. (2017). Controls on the Evolution of Ediacaran Metazoan Ecosystems: A Redox Perspective. *Geobiology* 15, 516–551. doi:10.1111/gbi.12232

Boyle, R. A., Clark, J. R., Poulton, S. W., Shields-Zhou, G., Canfield, D. E., and Lenton, T. M. (2013). Nitrogen Cycle Feedbacks as a Control on Euxinia in the Mid-proterozoic Ocean. *Nat. Commun.* 4, 1533. doi:10.1038/ncomms2511

Brocks, J. J., Jarrett, A. J. M., Sirantoine, E., Hallmann, C., Hoshino, Y., and Liyanage, T. (2017). The Rise of Algae in Cryogenian Oceans and the Emergence of Animals. *Nature* 548, 578–581. doi:10.1038/nature23457

Brunner, B., Contreras, S., Lehmann, M. F., Matantseva, O., Rollog, M., Kalvelage, T., et al. (2013). Nitrogen Isotope Effects Induced by Anammox Bacteria. *Proc. Natl. Acad. Sci.* 110, 18994–18999. doi:10.1073/pnas.1310488110

Caetano-Filho, S., Paula-Santos, G. M., Guacaneme, C., Babinski, M., Bedoya-Rueda, C., Peloso, M., et al. (2019). Sequence Stratigraphy and Chemostratigraphy of an Ediacaran-Cambrian Foreland-Related Carbonate Ramp (Bambuí Group, Brazil). *Precambrian Res.* 331, 105365. doi:10.1016/j.precamres.2019.105365

Caetano-Filho, S., Sansjofre, P., Ader, M., Paula-Santos, G. M., Guacaneme, C., Babinski, M., et al. (2021). A Large Epeiric Methanogenic Bambuí Sea in the Core of Gondwana Supercontinent? *Geosci. Front.* 12, 203–218. doi:10.1016/j.gsf.2020.04.005

Calvert, S. E. (2004). Beware Intercepts: Interpreting Compositional Ratios in Multi-Component Sediments and Sedimentary Rocks. *Org. Geochem.* 35, 981–987. doi:10.1016/j.orggeochem.2004.03.001

Canfield, D. E., Glazer, A. N., and Falkowski, P. G. (2010). The Evolution and Future of Earth's Nitrogen Cycle. *Science* 330, 192–196. doi:10.1126/science.1186120

Canfield, D. E. (2006). Models of Oxic Respiration, Denitrification and Sulfate Reduction in Zones of Coastal Upwelling. *Geochimica et Cosmochimica Acta* 70, 5753–5765. doi:10.1016/j.gca.2006.07.023

Casciotti, K. L. (2009). Inverse Kinetic Isotope Fractionation During Bacterial Nitrite Oxidation. *Geochimica et Cosmochimica Acta* 73, 2061–2076. doi:10.1016/j.gca.2008.12.022

Caxito, F. A., Frei, R., Uhlein, G. J., Gonçalves Dias, T., Árting, T. B., and Uhlein, A. (2018). Multiproxy Geochemical and Isotope Stratigraphy Records of a Neoproterozoic Oxygenation Event in the Ediacaran Sete Lagoas Cap Carbonate, Bambuí Group, Brazil. *Chem. Geology.* 481, 119–132. doi:10.1016/j.chemgeo.2018.02.007

Caxito, F. d. A., Halverson, G. P., Uhlein, A., Stevenson, R., Gonçalves Dias, T., Uhlein, G. J., et al. (2012). Marinoan Glaciation in East Central Brazil. *Precambrian Res.* 200-203, 38–58. doi:10.1016/j.precamres.2012.01.005

Chen, Y., Diamond, C. W., Stüeken, E. E., Cai, C., Gill, B. C., Zhang, F., et al. (2019). Coupled Evolution of Nitrogen Cycling and Redoxcline Dynamics on the Yangtze Block Across the Ediacaran-Cambrian Transition. *Geochimica et Cosmochimica Acta* 257, 243–265. doi:10.1016/j.gca.2019.05.017

Costa, M. T., and Branco, J. J. R. (1961). "Roteiro para a excursão Belo Horizonte - Brasília," in *Anais do Congresso Brasileiro de Geologia*. Editor J. J. R. Branco (Belo Horizonte: SBG), 1–119.

Cox, G. M., Sansjofre, P., Blades, M. L., Farkas, J., and Collins, A. S. (2019). Dynamic Interaction Between Basin Redox and the Biogeochemical Nitrogen Cycle in an Unconventional Proterozoic Petroleum System. *Sci. Rep.* 9, 5200. doi:10.1038/s41598-019-40783-4

Cremonese, L., Shields-Zhou, G., Struck, U., Ling, H.-F., Och, L., Chen, X., et al. (2013). Marine Biogeochemical Cycling During the Early Cambrian Constrained by a Nitrogen and Organic Carbon Isotope Study of the Xiaotan Section, South China. *Precambrian Res.* 225, 148–165. doi:10.1016/j.precamres.2011.12.004

Crockford, P. W., Wing, B. A., Paytan, A., Hodgskiss, M. S. W., Mayfield, K. K., Hayles, J. A., et al. (2019). Barium-isotopic Constraints on the Origin of Post-Marinoan Barites. *Earth Planet. Sci. Lett.* 519, 234–244. doi:10.1016/j.epsl.2019.05.018

Cui, H., Warren, L. V., Uhlein, G. J., Okubo, J., Liu, X.-M., Plummer, R. E., et al. (2020). Global or Regional? Constraining the Origins of the Middle Bambuí Carbon Cycle Anomaly in Brazil. *Precambrian Res.* 348, 105861. doi:10.1016/j.precamres.2020.105861

Dardenne, M. A. (1978). "Síntese sobre a estratigrafia Do Grupo Bambuí no Brasil Central," in Proceedings of the 30th Congresso Brasileiro de Geologia, November, 1978 (Recife: SBG), 507–610.

Delpomdor, F. R. A., Ilambwetsi, A. M., Caxito, F. A., and Pedrosa-Soares, A. C. (2020). New Interpretation of the Basal Bambuí Group, Sete Lagoas High (Minas Gerais, E Brazil) by Sedimentological Studies and Regional Implications for the Aftermath of the Marinoan Glaciation: Correlations Across Brazil and Central Africa. *Geol. Belg.* 23, 1–17. doi:10.20341/gb.2019.010

Dong, L. F., Sobey, M. N., Smith, C. J., Rusmana, I., Phillips, W., Stott, A., et al. (2011). Dissimilatory Reduction of Nitrate to Ammonium, Not Denitrification

or Anammox, Dominates Benthic Nitrate Reduction in Tropical Estuaries. *Limnol. Oceanogr.* 56, 279–291. doi:10.4319/lo.2011.56.1.0279

Edwards, A. M., Platt, T., and Sathyendranath, S. (2004). The High-Nutrient, Low-Chlorophyll Regime of the Ocean: Limits on Biomass and Nitrate Before and After Iron Enrichment. *Ecol. Model.* 171, 103–125. doi:10.1016/j.ecolmodel.2003.06.001

Fawcett, S. E., Lomas, M. W., Casey, J. R., Ward, B. B., and Sigman, D. M. (2011). Assimilation of Upwelled Nitrate by Small Eukaryotes in the Sargasso Sea. *Nat. Geosci* 4, 717–722. doi:10.1038/ngeo1265

Fogel, M. L., and Cifuentes, L. A. (1993). "Isotope Fractionation During Primary Production," in *Organic Geochemistry*. Editors M. H. Engel and S. A. Macko (Boston, MA: Springer), 73–98. doi:10.1007/978-1-4615-2890-6_3

Füssel, J., Lam, P., Lavik, G., Jensen, M. M., Holtappels, M., Günter, M., et al. (2012). Nitrite Oxidation in the Namibian Oxygen Minimum Zone. *ISME J.* 6, 1200–1209. doi:10.1038/ismej.2011.178

Gallon, J. R. (1981). The Oxygen Sensitivity of Nitrogenase: A Problem for Biochemists and Micro-organisms. *Trends Biochem. Sci.* 6, 19–23. doi:10.1016/0968-0004(81)90008-6

Glass, J. B., Wolfe-Simon, F., and Anbar, A. D. (2009). Coevolution of Metal Availability and Nitrogen Assimilation in Cyanobacteria and Algae. *Geobiology* 7, 100–123. doi:10.1111/j.1472-4669.2009.00190.x

Godfrey, L. V., and Falkowski, P. G. (2009). The Cycling and Redox State of Nitrogen in the Archaean Ocean. *Nat. Geosci* 2, 725–729. doi:10.1038/ngeo633

Granger, J., Sigman, D. M., Lehmann, M. F., and Tortell, P. D. (2008). Nitrogen and Oxygen Isotope Fractionation During Dissimilatory Nitrate Reduction by Denitrifying Bacteria. *Limnol. Oceanogr.* 53, 2533–2545. doi:10.4319/lo.2008.53.6.2533

Granger, J., Sigman, D. M., Rohde, M. M., Maldonado, M. T., and Tortell, P. D. (2010). N and O Isotope Effects During Nitrate Assimilation by Unicellular Prokaryotic and Eukaryotic Plankton Cultures. *Geochimica et Cosmochimica Acta* 74, 1030–1040. doi:10.1016/j.gca.2009.10.044

Greenfield, L. G. (1992). Acid Hydrolysis and the Release of Fixed Ammonium From Soils. *Soil Biol. Biochem.* 24, 271–273. doi:10.1016/0038-0717(92)90229-Q

Grotzinger, J. P., Bowring, S. A., Saylor, B. Z., and Kaufman, A. J. (1995). Biostratigraphic and Geochronologic Constraints on Early Animal Evolution. *Science* 270, 598–604. doi:10.1126/science.270.5236.598

Guacaneme, C., Babinski, M., Paula-Santos, G. M. d., and Pedrosa-Soares, A. C. (2017). C, O, and Sr Isotopic Variations in Neoproterozoic-Cambrian Carbonate Rocks from Sete Lagoas Formation (Bambuí Group), in the Southern São Francisco Basin, Brazil. *Braz. J. Geol.* 47, 521–543. doi:10.1590/2317-4889201720160126

Haug, G. H., Pedersen, T. F., Sigman, D. M., Calvert, S. E., Nielsen, B., and Peterson, L. C. (1998). Glacial/interglacial Variations in Production and Nitrogen Fixation in the Cariaco Basin During the Last 580 Kyr. *Paleoceanography* 13, 427–432. doi:10.1029/98PA01976

Hippertt, J. P., Caxito, F. A., Uhlein, G. J., Nalini, H. A., Sial, A. N., Abreu, A. T., et al. (2019). The Fate of a Neoproterozoic Intracratonic Marine Basin: Trace Elements, TOC and IRON Speciation Geochemistry of the Bambuí Basin, Brazil. *Precambrian Res.* 330, 101–120. doi:10.1016/j.precamres.2019.05.001

Hoch, M. P., Fogel, M. L., and Kirchman, D. L. (1992). Isotope Fractionation Associated with Ammonium Uptake by a Marine Bacterium. *Limnol. Oceanogr.* 37, 1447–1459. doi:10.4319/lo.1992.37.7.1447

Iglesias, M., and Uhlein, A. (2009). Estratigrafia Do Grupo Bambuí e coberturas fanerozóicas no vale Do rio São Francisco, norte de Minas Gerais. *RBG* 39, 256–266. doi:10.25249/0375-7536.2009392256266

Ingall, E., and Jahnke, R. (1997). Influence of Water-Column Anoxia on the Elemental Fractionation of Carbon and Phosphorus During Sediment Diagenesis. *Mar. Geology.* 139, 219–229. doi:10.1016/S0025-3227(96)00112-0

Irwin, A. J., Finkel, Z. V., Schofield, O. M. E., and Falkowski, P. G. (2006). Scaling-up from Nutrient Physiology to the Size-Structure of Phytoplankton Communities. *J. Plankton Res.* 28, 459–471. doi:10.1093/plankt/fbi148

Iyer, S., Babinski, M., Krouse, H., and Chemalejr, F., Jr (1995). Highly 13C-Enriched Carbonate and Organic Matter in the Neoproterozoic Sediments of the BambuíGroup, Brazil. *Precambrian Res.* 73, 271–282. doi:10.1016/0301-9268(94)00082-3

Jensen, M. M., Lam, P., Revsbech, N. P., Nagel, B., Gaye, B., Jetten, M. S., et al. (2011). Intensive Nitrogen Loss over the Omani Shelf Due to Anammox Coupled with Dissimilatory Nitrite Reduction to Ammonium. *ISME J.* 5, 1660–1670. doi:10.1038/ismej.2011.44

Kessler, A. J., Bristow, L. A., Cardenas, M. B., Glud, R. N., Thamdrup, B., and Cook, P. L. M. (2014). The Isotope Effect of Denitrification in Permeable Sediments. *Geochimica et Cosmochimica Acta* 133, 156–167. doi:10.1016/j.gca.2014.02.029

Kikumoto, R., Tahata, M., Nishizawa, M., Sawaki, Y., Maruyama, S., Shu, D., et al. (2014). Nitrogen Isotope Chemostratigraphy of the Ediacaran and Early Cambrian Platform Sequence at Three Gorges, South China. *Gondwana Res.* 25, 1057–1069. doi:10.1016/j.gr.2013.06.002

Kuchenbecker, M., Atman, D., Costa, R. D. d., Pedrosa-Soares, A., and Babinski, M. (2016a). A Formação Gorutuba: sedimentação litorânea a continental na margem leste da Bacia Bambuí (MG). *Geol. USP. Sér. Cient.* 16, 67. doi:10.11606//issn.2316-9095.v16i2p67-81

Kuchenbecker, M., Babinski, M., Pedrosa-Soares, A. C., Lopes-Silva, L., and Pimenta, F. (2016b). Chemostratigraphy of the Lower Bambuí Group, Southwestern São Francisco Craton, Brazil: Insights on Gondwana Paleoenvironments. *Braz. J. Geol.* 46, 145–162. doi:10.1590/2317-488920160030285

Kuchenbecker, M., Costa, R. D. d., Babinski, M., Pedrosa-Soares, A. C., Lopes-Silva, L., and Pimenta, F. (2013). Proveniência e análise sedimentar da porção basal Do Grupo Bambuí em Arcos (MG). *Geol. Usp, Sér. Cient.* 13, 49–61. doi:10.5327/Z1519-874X201300040003

Kuchenbecker, M., Lopes-Silva, L., Pimenta, F., Pedrosa-Soares, A. C., and Babinski, M. (2011). Estratigrafia da porção basal Do grupo Bambuí na região de Arcos (MG): uma contribuição a partir de testemunhos de sondagem. *Geol. Usp, Sér. Cient.* 11, 45–54. doi:10.5327/Z1519-874X2011000200003

Kuchenbecker, M., Pedrosa-Soares, A. C., Babinski, M., Reis, H. L. S., Atman, D., and Costa, R. D. d. (2020). Towards an Integrated Tectonic Model for the Interaction Between the Bambuí basin and the Adjoining Orogenic Belts: Evidences from the Detrital Zircon Record of Syn-Orogenic Units. *J. South Am. Earth Sci.* 104, 102831. doi:10.1016/j.jsames.2020.102831

Lehmann, M. F., Bernasconi, S. M., Barbieri, A., and McKenzie, J. A. (2002). Preservation of Organic Matter and Alteration of its Carbon and Nitrogen Isotope Composition during Simulated and In Situ Early Sedimentary Diagenesis. *Geochimica et Cosmochimica Acta* 66, 3573–3584. doi:10.1016/S0016-7037(02)00968-7

Lenton, T. M., Boyle, R. A., Poulton, S. W., Shields-Zhou, G. A., and Butterfield, N. J. (2014). Co-evolution of Eukaryotes and Ocean Oxygenation in the Neoproterozoic Era. *Nat. Geosci* 7, 257–265. doi:10.1038/ngeo2108

Li, L., Lollar, B. S., Li, H., Wortmann, U. G., and Lacrampe-Couloume, G. (2012). Ammonium Stability and Nitrogen Isotope Fractionations for -NH3(aq)-NH3(gas) Systems at 20-70°C and pH of 2-13: Applications to Habitability and Nitrogen Cycling in Low-Temperature Hydrothermal Systems. *Geochimica et Cosmochimica Acta* 84, 280–296. doi:10.1016/j.gca.2012.01.040

Liu, K.-K., Kao, S.-J., Chiang, K.-P., Gong, G.-C., Chang, J., Cheng, J.-S., et al. (2013). Concentration Dependent Nitrogen Isotope Fractionation during Ammonium Uptake by Phytoplankton under an Algal Bloom Condition in the Danshuei Estuary, Northern Taiwan. *Mar. Chem.* 157, 242–252. doi:10.1016/j.marchem.2013.10.005

Liu, Y., Magnall, J. M., Gleeson, S. A., Bowyer, F., Poulton, S. W., and Zhang, J. (2020). Spatio-temporal Evolution of Ocean Redox and Nitrogen Cycling in the Early Cambrian Yangtze Ocean. *Chem. Geology.* 554, 119803. doi:10.1016/j.chemgeo.2020.119803

Martins, M., and Lemos, V. B. (2007). Análise estratigráfica das seqüências neoproterozóicas da Bacia Do São Francisco. *RBG* 37, 156–167. doi:10.25249/0375-7536.200737S4156167

Martins-Neto, M. A., and Hercos, C. M. (2002). "Sedimentation and Tectonic Setting of Early Neoproterozoic Glacial Deposits in South-Eastern Brazil," in *Precambrian Sedimentary Environments*. Editors W. Altermann and P. L. Corcoran (Oxford, UK: Blackwell Publishing Ltd.), 383–403. doi:10.1002/9781444304312.ch18

Martins-Neto, M. A., Pedrosa-Soares, A. C., and Lima, S. A. A. (2001). Tectono-sedimentary Evolution of Sedimentary Basins from Late Paleoproterozoic to Late Neoproterozoic in the São Francisco Craton and Araçuaí Fold belt, Eastern Brazil. *Sediment. Geology.* 141-142, 343–370. doi:10.1016/S0037-0738(01)00082-3

Martins-Neto, M. A. (2009). Sequence Stratigraphic Framework of Proterozoic Successions in Eastern Brazil. *Mar. Pet. Geology.* 26, 163–176. doi:10.1016/j.marpetgeo.2007.10.001

McCready, R. G. L., Gould, W. D., and Barendregt, R. W. (1983). Nitrogen Isotope Fractionation During the Reduction of NO3− to NH4+ by Desulfovibrio Sp. *Can. J. Microbiol.* 29, 231–234. doi:10.1139/m83-038

Meija, J., Coplen, T. B., Berglund, M., Brand, W. A., De Bièvre, P., Gröning, M., et al. (2016). Isotopic Compositions of the Elements 2013 (IUPAC Technical Report). *Pure Appl. Chem.* 88, 293–306. doi:10.1515/pac-2015-0503

Meyer, K. M., Ridgwell, A., and Payne, J. L. (2016). The Influence of the Biological Pump on Ocean Chemistry: Implications for Long-term Trends in Marine Redox Chemistry, the Global Carbon Cycle, and Marine Animal Ecosystems. *Geobiology* 14, 207–219. doi:10.1111/gbi.12176

Mills, D. B., Ward, L. M., Jones, C., Sweeten, B., Forth, M., Treusch, A. H., et al. (2014). Oxygen Requirements of the Earliest Animals. *Proc. Natl. Acad. Sci.* 111, 4168–4172. doi:10.1073/pnas.1400547111

Möbius, J. (2013). Isotope Fractionation During Nitrogen Remineralization (Ammonification): Implications for Nitrogen Isotope Biogeochemistry. *Geochimica et Cosmochimica Acta* 105, 422–432. doi:10.1016/j.gca.2012.11.048

Morales, L. V., Granger, J., Chang, B. X., Prokopenko, M. G., Plessen, B., Gradinger, R., et al. (2014). Elevated 15N/14N in Particulate Organic Matter, Zooplankton, and Diatom Frustule-Bound Nitrogen in the Ice-Covered Water Column of the Bering Sea Eastern Shelf. *Deep Sea Res. Part Topical Stud. Oceanography* 109, 100–111. doi:10.1016/j.dsr2.2014.05.008

Moreira, D. S., Uhlein, A., Dussin, I. A., Uhlein, G. J., and Pimentel Misuzaki, A. M. (2020). A Cambrian Age for the Upper Bambuí Group, Brazil, Supported by the First U-Pb Dating of Volcaniclastic Bed. *J. South Am. Earth Sci.* 99, 102503. doi:10.1016/j.jsames.2020.102503

Müller, P. J. (1977). Ratios in Pacific Deep-Sea Sediments: Effect of Inorganic Ammonium and Organic Nitrogen Compounds Sorbed by Clays. *Geochimica et Cosmochimica Acta* 41, 765–776. doi:10.1016/0016-7037(77)90047-3

Nursall, J. R. (1959). Oxygen as a Prerequisite to the Origin of the Metazoa. *Nature* 183, 1170–1172. doi:10.1038/1831170b0

Okubo, J., Muscente, A. D., Luvizotto, G. L., Uhlein, G. J., and Warren, L. V. (2018). Phosphogenesis, Aragonite Fan Formation and Seafloor Environments Following the Marinoan Glaciation. *Precambrian Res.* 311, 24–36. doi:10.1016/j.precamres.2018.04.002

Okubo, J., Warren, L. V., Luvizotto, G. L., Varejão, F. G., Quaglio, F., Uhlein, G. J., et al. (2020). Evidences of Seismic Events During the Sedimentation of Sete Lagoas Formation (Bambuí Group - Ediacaran, Brazil). *J. South Am. Earth Sci.* 98, 102461. doi:10.1016/j.jsames.2019.102461

Paula-Santos, G. M., Babinski, M., Kuchenbecker, M., Caetano-Filho, S., Trindade, R. I., and Pedrosa-Soares, A. C. (2015). New Evidence of an Ediacaran Age for the Bambuí Group in Southern São Francisco Craton (Eastern Brazil) from Zircon U-Pb Data and Isotope Chemostratigraphy. *Gondwana Res.* 28, 702–720. doi:10.1016/j.gr.2014.07.012

Paula-Santos, G. M., Caetano-Filho, S., Babinski, M., and Enzweiler, J. (2018). Rare Earth Elements of Carbonate Rocks from the Bambuí Group, Southern São Francisco Basin, Brazil, and Their Significance as Paleoenvironmental Proxies. *Precambrian Res.* 305, 327–340. doi:10.1016/j.precamres.2017.12.023

Paula-Santos, G. M., Caetano-Filho, S., Babinski, M., Trindade, R. I. F., and Guacaneme, C. (2017). Tracking Connection and Restriction of West Gondwana São Francisco Basin Through Isotope Chemostratigraphy. *Gondwana Res.* 42, 280–305. doi:10.1016/j.gr.2016.10.012

Paula-Santos, G. M., Caetano-Filho, S., Enzweiler, J., Navarro, M. S., Babinski, M., Guacaneme, C., et al. (2020). Rare Earth Elements in the Terminal Ediacaran Bambuí Group Carbonate Rocks (Brazil): Evidence for High Seawater Alkalinity during Rise of Early Animals. *Precambrian Res.* 336, 105506. doi:10.1016/j.precamres.2019.105506

Paula-Santos, G. M. d., and Babinski, M. (2018). Sedimentary Provenance in the Southern Sector of the São Francisco Basin, SE Brazil. *Braz. J. Geol.* 48, 51–74. doi:10.1590/2317-4889201820170061

Pennock, J. R., Velinsky, D. J., Ludlam, J. M., Sharp, J. H., and Fogel, M. L. (1996). Isotopic Fractionation of Ammonium and Nitrate during Uptake by Skeletonema Costatum : Implications for δ15N Dynamics Under Bloom Conditions. *Limnol. Oceanogr.* 41, 451–459. doi:10.4319/lo.1996.41.3.0451

Perrella Júnior, P., Uhlein, A., Uhlein, G. J., Sial, A. N., Pedrosa-Soares, A. C., and Lima, O. N. B. d. (2017). Facies Analysis, Sequence Stratigraphy and Chemostratigraphy of the Sete Lagoas Formation (Bambui Group), Northern Minas Gerais State, Brazil: Evidence of a Cap Carbonate Deposited on the Januária Basement High. *Braz. J. Geol.* 47, 59–77. doi:10.1590/2317-4889201720160112

Quan, T. M., Wright, J. D., and Falkowski, P. G. (2013). Co-variation of Nitrogen Isotopes and Redox States Through Glacial-Interglacial Cycles in the Black Sea. *Geochimica et Cosmochimica Acta* 112, 305–320. doi:10.1016/j.gca.2013.02.029

Reis, H. L. S., and Alkmim, F. F. (2015). Anatomy of a Basin-controlled Foreland Fold-Thrust Belt Curve: The Três Marias Salient, São Francisco Basin, Brazil. *Mar. Pet. Geology.* 66, 711–731. doi:10.1016/j.marpetgeo.2015.07.013

Reis, H. L. S., Suss, J. F., Fonseca, R. C. S., and Alkmim, F. F. (2017). Ediacaran Forebulge Grabens of the Southern São Francisco Basin, SE Brazil: Craton Interior Dynamics During West Gondwana Assembly. *Precambrian Res.* 302, 150–170. doi:10.1016/j.precamres.2017.09.023

Reis, H. L. S., and Suss, J. F. (2016). Mixed Carbonate-Siliciclastic Sedimentation in Forebulge Grabens: An Example from the Ediacaran Bambuí Group, São Francisco Basin, Brazil. *Sediment. Geology.* 339, 83–103. doi:10.1016/j.sedgeo.2016.04.004

Sanchez, E. A. M., Uhlein, A., and Fairchild, T. R. (2021). Treptichnus Pedum in the Três Marias Formation, South-central Brazil, and its Implications for the Ediacaran-Cambrian Transition in South America. *J. South Am. Earth Sci.* 105, 102983. doi:10.1016/j.jsames.2020.102983

Santos, R. V., Souza de Alvarenga, C. J., Babinski, M., Ramos, M. L. S., Cukrov, N., Fonseca, M. A., et al. (2004). Carbon Isotopes of Mesoproterozoic-Neoproterozoic Sequences from Southern São Francisco Craton and Araçuaí Belt, Brazil: Paleographic Implications. *J. South Am. Earth Sci.* 18, 27–39. doi:10.1016/j.jsames.2004.08.009

Schimmelmann, A., Mastalerz, M., Gao, L., Sauer, P. E., and Topalov, K. (2009). Dike Intrusions into Bituminous Coal, Illinois Basin: H, C, N, O Isotopic Responses to Rapid and Brief Heating. *Geochimica et Cosmochimica Acta* 73, 6264–6281. doi:10.1016/j.gca.2009.07.027

Seefeldt, L. C., Hoffman, B. M., and Dean, D. R. (2009). Mechanism of Mo-dependent Nitrogenase. *Annu. Rev. Biochem.* 78, 701–722. doi:10.1146/annurev.biochem.78.070907.103812

Seer, H. J., Moraes, L. C., and Fogaça, A. C. C. (1989). *Roteiro Geológico para a região de Lagoa Formosa-Chumbo-Carmo do Paranaíba, MG*. Belo Horizonte: SBG/MG.

Sigman, D. M., Altabet, M. A., McCorkle, D. C., Francois, R., and Fischer, G. (1999). The δ15N of Nitrate in the Southern Ocean: Consumption of Nitrate in Surface Waters. *Glob. Biogeochem. Cycles* 13, 1149–1166. doi:10.1029/1999GB900038

Sigman, D. M., and Fripiat, F.. (2019). Nitrogen Isotopes in the Ocean. *Encyclopedia of Ocean Sciences* 1, 263–278. doi:10.1016/B978-0-12-409548-9.11605-7

Sperling, E. A., Frieder, C. A., Raman, A. V., Girguis, P. R., Levin, L. A., and Knoll, A. H. (2013). Oxygen, Ecology, and the Cambrian Radiation of Animals. *Proc. Natl. Acad. Sci. U S A.* 110, 13446–13451. doi:10.1073/pnas.1312778110

Stüeken, E. E., Buick, R., and Schauer, A. J. (2015). Nitrogen Isotope Evidence for Alkaline Lakes on Late Archean Continents. *Earth Planet. Sci. Lett.* 411, 1–10. doi:10.1016/j.epsl.2014.11.037

Stüeken, E. E., Kipp, M. A., Koehler, M. C., and Buick, R. (2016). The Evolution of Earth's Biogeochemical Nitrogen Cycle. *Earth-Science Rev.* 160, 220–239. doi:10.1016/j.earscirev.2016.07.007

Stüeken, E. E., Zaloumis, J., Meixnerová, J., and Buick, R. (2017). Differential Metamorphic Effects on Nitrogen Isotopes in Kerogen Extracts and Bulk Rocks. *Geochimica et Cosmochimica Acta* 217, 80–94. doi:10.1016/j.gca.2017.08.019

Sun, Y. D., Zulla, M. J., Joachimski, M. M., Bond, D. P. G., Wignall, P. B., Zhang, Z. T., et al. (2019). Ammonium Ocean Following the End-Permian Mass Extinction. *Earth Planet. Sci. Lett.* 518, 211–222. doi:10.1016/j.epsl.2019.04.036

Tesdal, J.-E., Galbraith, E. D., and Kienast, M. (2013). Nitrogen Isotopes in Bulk Marine Sediment: Linking Seafloor Observations with Subseafloor Records. *Biogeosciences* 10, 101–118. doi:10.5194/bg-10-101-2013

Thomazo, C., Ader, M., and Philippot, P. (2011). Extreme 15N-Enrichments in 2.72-Gyr-Old Sediments: Evidence for a Turning Point in the Nitrogen Cycle. *Geobiology* 9, 107–120. doi:10.1111/j.1472-4669.2011.00271.x

Thomazo, C., and Papineau, D. (2013). Biogeochemical Cycling of Nitrogen on the Early Earth. *Elements* 9, 345–351. doi:10.2113/gselements.9.5.345

Tyrrell, T. (1999). The Relative Influences of Nitrogen and Phosphorus on Oceanic Primary Production. *Nature* 400, 525–531. doi:10.1038/22941

Uhlein, A., Baptista, M. C., Seer, H. J., Caxito, F. de. A., Uhlein, G. J., and Dardenne, M. A. (2011). A Formação Lagoa Formosa, Grupo Bambuí (MG): Sistema Deposicional De Leque Submarino Em Bacia De Ante-país. *Geonomos* 19 (2), 163–172. doi:10.18285/geonomos.v19i2.51

Uhlein, G. J., Uhlein, A., Halverson, G. P., Stevenson, R., Caxito, F. A., Cox, G. M., et al. (2016). The Carrancas Formation, Bambuí Group: A Record of Pre-marinoan Sedimentation on the Southern São Francisco Craton, Brazil. *J. South Am. Earth Sci.* 71, 1–16. doi:10.1016/j.jsames.2016.06.009

Uhlein, G. J., Uhlein, A., Pereira, E., Caxito, F. A., Okubo, J., Warren, L. V., et al. (2019). Ediacaran Paleoenvironmental Changes Recorded in the Mixed Carbonate-Siliciclastic Bambuí Basin, Brazil. *Palaeogeogr. Palaeoclimatol. Palaeoecol.* 517, 39–51. doi:10.1016/j.palaeo.2018.12.022

Uhlein, G. J., Uhlein, A., Stevenson, R., Halverson, G. P., Caxito, F. A., and Cox, G. M. (2017). Early to Late Ediacaran Conglomeratic Wedges from a Complete Foreland Basin Cycle in the Southwest São Francisco Craton, Bambuí Group, Brazil. *Precambrian Res.* 299, 101–116. doi:10.1016/j.precamres.2017.07.020

Van Cappellen, P., and Ingall, E. D. (1994). Benthic Phosphorus Regeneration, Net Primary Production, and Ocean Anoxia: A Model of the Coupled Marine Biogeochemical Cycles of Carbon and Phosphorus. *Paleoceanography* 9, 677–692. doi:10.1029/94PA01455

Vieira, L. C., Almeida, R. P., Trindade, R. I. F., Nogueira, A. C. R., and Janikian, L. (2007a). A Formação Sete Lagoas em sua área-tipo: fácies, estratigrafia e sistemas deposicionais. *RBG* 37, 1–14. doi:10.25249/0375-7536.200737S4114

Vieira, L. C., Trindade, R. I. F., Nogueira, A. C. R., and Ader, M. (2007b). Identification of a Sturtian Cap Carbonate in the Neoproterozoic Sete Lagoas Carbonate Platform, Bambuí Group, Brazil. *Comptes Rendus Geosci.* 339, 240–258. doi:10.1016/j.crte.2007.02.003

Wang, D., Struck, U., Ling, H.-F., Guo, Q.-J., Shields-Zhou, G. A., Zhu, M.-Y., et al. (2015). Marine Redox Variations and Nitrogen Cycle of the Early Cambrian Southern Margin of the Yangtze Platform, South China: Evidence from Nitrogen and Organic Carbon Isotopes. *Precambrian Res.* 267, 209–226. doi:10.1016/j.precamres.2015.06.009

Wang, X., Jiang, G., Shi, X., Peng, Y., and Morales, D. C. (2018). Nitrogen Isotope Constraints on the Early Ediacaran Ocean Redox Structure. *Geochimica et Cosmochimica Acta* 240, 220–235. doi:10.1016/j.gca.2018.08.034

Warren, L. V., Quaglio, F., Riccomini, C., Simões, M. G., Poiré, D. G., Strikis, N. M., et al. (2014). The Puzzle Assembled: Ediacaran Guide Fossil Cloudina Reveals an Old Proto-Gondwana Seaway. *Geology* 42, 391–394. doi:10.1130/G35304.1

Wood, R. A., Poulton, S. W., Prave, A. R., Hoffmann, K.-H., Clarkson, M. O., Guilbaud, R., et al. (2015). Dynamic Redox Conditions Control Late Ediacaran Metazoan Ecosystems in the Nama Group, Namibia. *Precambrian Res.* 261, 252–271. doi:10.1016/j.precamres.2015.02.004

Wood, R., Donoghue, P. C. J., Lenton, T. M., Liu, A. G., and Poulton, S. W. (2020). The Origin and Rise of Complex Life: Progress Requires Interdisciplinary Integration and Hypothesis Testing. *Interf. Focus.* 10, 20200024. doi:10.1098/rsfs.2020.0024

Wood, R., Liu, A. G., Bowyer, F., Wilby, P. R., Dunn, F. S., Kenchington, C. G., et al. (2019). Integrated Records of Environmental Change and Evolution Challenge the Cambrian Explosion. *Nat. Ecol. Evol.* 3, 528–538. doi:10.1038/s41559-019-0821-6

Xiang, L., Schoepfer, S. D., Zhang, H., Cao, C.-q., and Shen, S.-z. (2018). Evolution of Primary Producers and Productivity Across the Ediacaran-Cambrian Transition. *Precambrian Res.* 313, 68–77. doi:10.1016/j.precamres.2018.05.023

Xu, D., Wang, X., Shi, X., Tang, D., Zhao, X., Feng, L., et al. (2020). Nitrogen Cycle Perturbations Linked to Metazoan Diversification During the Early Cambrian. *Palaeogeogr. Palaeoclimatol. Palaeoecol.* 538, 109392. doi:10.1016/j.palaeo.2019.109392

Yang, Y., Wang, Y., Zhang, Z., Wang, W., Ren, X., Gao, Y., et al. (2018). Diurnal and Seasonal Variations of Thermal Stratification and Vertical Mixing in a Shallow Fresh Water Lake. *J. Meteorol. Res.* 32, 219–232. doi:10.1007/s13351-018-7099-5

Zerkle, A. L. (2005). Biogeochemical Signatures through Time as Inferred from Whole Microbial Genomes. *Am. J. Sci.* 305, 467–502. doi:10.2475/ajs.305.6-8.467

Zhang, X., Sigman, D. M., Morel, F. M. M., and Kraepiel, A. M. L. (2014). Nitrogen Isotope Fractionation by Alternative Nitrogenases and Past Ocean Anoxia. *Proc. Natl. Acad. Sci. USA* 111, 4782–4787. doi:10.1073/pnas.1402976111

Conflict of Interest: The authors declare that the research was conducted in the absence of any commercial or financial relationships that could be construed as a potential conflict of interest.

Publisher's Note: All claims expressed in this article are solely those of the authors and do not necessarily represent those of their affiliated organizations, or those of the publisher, the editors and the reviewers. Any product that may be evaluated in this article, or claim that may be made by its manufacturer, is not guaranteed or endorsed by the publisher.

Copyright © 2021 Fraga-Ferreira, Ader, Caetano-Filho, Sansjofre, Paula-Santos, Babinski, Guacaneme, Bedoya-Rueda, Rojas, Reis, Kuchenbecker and Trindade. This is an open-access article distributed under the terms of the Creative Commons Attribution License (CC BY). The use, distribution or reproduction in other forums is permitted, provided the original author(s) and the copyright owner(s) are credited and that the original publication in this journal is cited, in accordance with accepted academic practice. No use, distribution or reproduction is permitted which does not comply with these terms.